NTNU

Norwegian University of
Science and Technology

Investigation of Electrical Properties of a new low-GWP Insulation Gas

Comparison of AirPlus and Synthetic Air

Ruben Mong

Master of Energy and Environmental Engineering
Submission date: June 2018
Supervisor: Frank Mauseth, IEL
Co-supervisor: Atle Pedersen, SINTEF Energy Research
Nina Sasaki Støa-Aanensen, SINTEF Energy Research

Norwegian University of Science and Technology
Department of Electric Power Engineering

Preface

This master's thesis is a contribution to an independent investigation of electrical properties of the new AirPlus (C5 Perfluoroketone) gas which could replace SF6 as an insulation gas in medium-voltage insulation equipment. The thesis presents observations for AirPlus and a comparison with synthetic air using the up-and-down method with lightning impulses.

I would like to thank my supervisors associate professor Frank Mauseth (NTNU), Atle Pedersen (Sintef Energy Research), and Nina Sasaki Støa-Aanesen (Sintef Energy Research) for invaluable guidance and help, and for always being available when needed.

Ruben Mong, Trondheim, June 2018.

Abstract

Sulfur hexafluoride (SF_6) is a widely used insulation gas in medium- to high-voltage equipment due to its excellent dielectric properties. It has however one important weakness; a large global warming potential (GWP) of 23,900 CO_2-equivalents, making it a target for phase out by legislative entities such as the European Union. This report will investigate a new potential low-GWP gas to replace SF_6 in medium-voltage equipment called AirPlus, a combination of 7.5% synthetic air and 92.5 % C_5 Perfluoroketone (C_5 PFK).

To test the dielectric performance of AirPlus, the up-and-down method is used with a standard lightning impulse (LI) as voltage stress and 1 minute waiting time between each application. The method provides an estimate for the 50% breakdown voltage and the standard deviation. AirPlus will be tested for gas pressure, gap length, electrode shape, and polarity. The pressure is chosen to 1.00 and 1.50 bar, and the gap length is adjusted between 10 and 80 mm. The electrode configurations are chosen to represent both inhomogeneous field distribution using a rod-plane gap, and a quasi-homogeneous field distribution using a plane-plane gap. The three rods used in the rod-plane gap have a hemispherical tip of radius 2.5, 5.0 and 10.0 mm.

In homogeneous fields, the results for the plane-plane gap showed negligible impact of LI polarity for both synthetic air and AirPlus. For the three rod-plane gaps, the inhomogeneous field distribution confirmed that synthetic air is most dependent on positive polarity, resulting in higher values for $U_{50\%}$ compared with negative polarity. AirPlus on the other hand is most dependent on negative polarity, sharing the same property as SF_6, resulting in higher values for $U_{50\%}$ compared with positive polarity. The difference between negative polarity and positive polarity in AirPlus is generally 7-10 kV or higher.

The study of inhomogeneity and breakdown voltage revealed that AirPlus could be more sensitive to increased inhomogeneity than synthetic air. The critical flashover voltage is 50% larger for AirPlus compared with synthetic air in homogeneous fields, but for inhomogeneous fields, the measured critical flashover voltage is only 30% larger in AirPlus compared with synthetic air.

Before changing a parameter, each test series was re-tested for the first gap length after performing the up-and-down method for all gap lengths. The re-testing resulted in an average increase of 10.6% for synthetic air and only 1.8% for AirPlus. The low impact of breakdowns is also reflected in the gas analysis of AirPlus which showed no indication of gas decomposition after 94 LI breakdowns at 1.50 bar.

For the scope of this project, AirPlus is an improvement from synthetic air and can be used for more compact protection designs. It is also beneficial that the critical flashover voltage in AirPlus is less affected by breakdowns than synthetic air. An important discovery is the potential reduced dielectric strength for increased field inhomogeneity caused by the shape of the electrodes, reducing the benefit of using AirPlus instead of synthetic air, from 50% to approximately 30%.

Sammendrag

Hensikten med prosjektet er å kartlegge dielektriske egenskaper til en ny miljøvennlig isolasjonsgass som potensielt kan erstatte SF_6 i mellomspenningsanlegg. Gassen som er gitt navnet AirPlus, er en blanding av 7.5% teknisk luft og 92.5% C_5 perfluoroketone. AirPlus har et globalt oppvarmingspotensial (GWP) på mindre enn 1 som er en stor forbedring sammenlignet med 23'900 GWP for SF_6.

I mellomspenning er lynimpulser og streameraktivitet viktige fenomener. AirPlus og teknisk luft er derfor testet for lynimpulser gjennom opp-ned metoden til Dixon og Mood med 31 repetisjoner for å teste de dielektriske egenskapene. Gassene er også testet for en rekke gapavstander mellom 10 og 80 mm, to forskjellige trykk (1.00 og 1.50 bar), positiv og negativ lynimpulspolaritet, og fire typer elektrodegap. Elektrodegapene representerer et homogent gap med plate-plate elektroder, og inhomogene gap ved spiss-plate. Spiss-plate gapene har tre forskjellige elektroder med halvkule som tupp. Disse har radius 2.5, 5.0, og 10.0 mm.

Resultatene viser at AirPlus er markant bedre enn teknisk luft for homogene gap med 50% større verdier for $U_{50\%}$ (50% gjennomslagsspenning). I mer inhomogene gap er forbedringen redusert til ca. 30%. AirPlus er også mer påvirket av negative lynimpulser som gir lavere $U_{50\%}$ enn for positive lynimpulser. Forskjellen mellom negativ og positiv lynimpuls er ca. 7-10 kV eller mere. AirPlus virker også å være en dielektrisk mer stabil gass enn teknisk luft.

Det første gapet som testes har blitt systematisk re-testet før andre parametere enn gapavstand endres. Disse testene viste at teknisk luft gir i snitt 10.6% høyere verdier for $U_{50\%}$ ved re-test sammenlignet med første måling. I AirPlus er økningen bare 1.8% fra første test til re-test. Kromatografisk analyse av AirPlus etter 94 gjennomslag viser få tegn til nedbrytning av syntetisk luft eller C_5 PFK.

For det som er undersøkt i prosjektet er AirPlus en forbedring sammenlignet med teknisk luft. Gassen vil kunne bidra til å lage mer kompakt vern av mellomspenningsanlegg enn det teknisk luft alene vil kunne gjøre.

Table of Contents

1 Introduction

The world is slowly adapting its behaviour in response to climate change. New technologies are sought to replace old and polluting ones. This also includes electrical insulation. SF_6 has been an excellent insulation gas in medium- and high-voltage equipment with three times the dielectric performance of air. Despite this, legislative entities such as the European Union are searching for alternative gases to replace SF_6 in medium voltage equipment. The motivation is the large global warming potential (GWP) of SF_6 at 23,900 CO_2-equivalents over a 100-year period, making SF_6 one of the six greenhouse gases listed in the Kyoto protocol (Houghton et al. 1995). As leakage is largely unavoidable, the best solution is currently to seek new gases to replace SF_6 (Hyrenbach and Zache 2016).

One such alternative is the newly developed C_5 Perfluoroketone (C_5 PFK) with chemical formula $C_5F_{10}O$, showing promise as a replacement to SF_6 with a GWP of 1 and excellent dielectric properties. The gas is also non-flammable, chemically stable, and non-toxic, all very useful properties for an insulation gas. The large limitation of C_5 PFK is the boiling point of 27°C, a value far too high for widespread use in applications such as gas-insulated switchgear which are used both indoors and outdoors (Kaveh Niayesh and Magne Runde 2017). It is therefore necessary to combine C_5 PFK with a carrier gas to reduce the boiling point to a level that is useful for electrical protection (Simka and Ranjan 2015). One such carrier gas could be synthetic air, named AirPlus when combined with C_5 PFK. This report will investigate the dielectric performance of AirPlus with a concentration of 7.5% C_5 PFK and 92.5% synthetic air (mole fraction) as well as synthetic air as an independent insulation gas to compare the dielectric strength of AirPlus and synthetic air.

In the range of medium-voltage to high-voltage systems up to about 230 kV, the most severe overvoltages are fast front overvoltages such as a lightning overvoltage. In this voltage range, streamers also play a significant role in protection of electrical equipment (White 2007). These events will therefore be key for examining the dielectric performance of AirPlus used to design insulation protection for medium voltage equipment such as switchgears.

The 50% breakdown voltage (critical flashover voltage) of the AirPlus mixture will be found using a standard 1.2/50 μs lightning impulse (LI) using the up-and-down method to give an indication of how the new gas performs compared with synthetic air. Each impulse is separated by 1 minute. The critical flashover voltage will be analysed for gap distance, gas pressure, field inhomogeneity, and LI polarity. For synthetic air, positive lightning impulses should result in the lowest breakdown voltage, while for the electronegative gas SF_6, negative lightning impulses will give the lowest breakdown voltage (Pedersen, Blaszczyk, and Boehme 2009). The potential impact of LI polarity in AirPlus is therefore an important result. To study the effect of field inhomogeneity, four different electrodes are used; one plane-type electrode to create a quasi-homogeneous field in a plane-plane gap, and three rods with hemispherical tips of varying radius in a rod-plane gap, resulting in an inhomogeneous field.

Numerical analysis of the streamer criterion in synthetic air will be performed to compare the measured values with theoretical values, and to determine the streamer mechanisms present for the test series.

In addition to the investigation of dielectric properties, AirPlus will also be tested for gas decomposition to investigate the potential introduction of by-products LI breakdowns for the 10 mm rod at 1.50 bar.

2 Electrical Breakdown in Gases

The Townsend mechanism is important for understanding electrical breakdowns in air. It describes how an insulator can become a good conductor for electrical current. It is on the other hand not adequate for avalanches containing around 10^8 electrons or more. This can occur when the gap distance, pressure, or electric field stress is increased. To explain breakdowns for electron avalanches of this size, the mechanism of streamers, or a channel of ionisation, must be used (Ildstad 2016).

2.1 Townsend mechanism

Townsend breakdown is an electron avalanche that reaches the anode (if the avalanche starts at the cathode), meaning that a very large number of electrons move from the cathode to the anode. To find the breakdown criterion, the number of electrons reaching the anode must therefore be calculated.

When particles (Ildstad 2016) are subjected to an external force through an electrical field, Coulomb forces will result in a net movement for the particles. Some of the moving particles will collide, releasing energy and, on some occasions, ionise the particles. The probability of such an ionisation by an electron per unit length is known as Townsend's first ionisation coefficient, α. This probability is a function of both field strength, E, and the inverse of pressure (i.e. the mean free path).

The ionisation from Townsend's first ionisation coefficient leads to a change in the number of free electrons, N_e, which for a distance x is given by the number of free electrons and the probability that these will ionise another particle

$$\mathrm{d}N_e = \alpha N_e(x)\mathrm{d}x \tag{2.1}$$

The boundary condition at the cathode is the number of electrons, N_{ec}, released per second. Integrating Eq. 2.1 from 0 to the gap distance d, the total number of electrons reaching the anode can be calculated, assuming a homogeneous field, using

$$N_e(d) = N_{ec}e^{\alpha d} \tag{2.2}$$

where $e^{\alpha d}$ is the electron avalanche created by the ionisation of particles (E. Kuffel, Zaegel, and J. Kuffel 2000).

The electrons released from the cathode in Eq. 2.2 are caused by bombardment by ions and photons after positive ions are generated. The probability of an electron being released from the cathode for a generated positive ion is known as Townsend's second ionisation coefficient, γ. Another source of electrons is the number of electrons generated by background conditions such as radiation, N_0. The number of electrons released from the cathode can then be found for a gap distance d using

$$N_{ec} = N_0 + \gamma N_{ec}(e^{\alpha d} - 1) \tag{2.3}$$

where $N_{ec}(e^{\alpha d} - 1)$ is the total number of generated positive ions for a given distance. Rearranging

Eq. 2.3 gives

$$N_{ec} = \frac{N_0}{1-\gamma(e^{\alpha d}-1)} \tag{2.4}$$

The total number of electrons reaching the anode per second using Eq. 2.1 and Eq. 2.2 then becomes

$$N_e = \frac{N_0 e^{\alpha d}}{1-\gamma(e^{\alpha d}-1)} \tag{2.5}$$

where i_0 is the circuit and gas independent current generated by background conditions.

The current through the gap can be found by multiplying Eq. 2.5 with the electron charge, leading to the approximation

$$i \approx \frac{i_0 e^{\alpha d}}{1-\gamma(e^{\alpha d}-1)} \tag{2.6}$$

Electrical breakdown is now found by setting the denominator to zero, resulting in an infinitely high current.

2.1.1 Electronegative gases

For electronegative gases such as SF_6, slow electrons can be caught to form negative ions. This will reduce the number of free electrons. The probability of one electron being caught per unit length is expressed as the attachment coefficient η. For such gases, the number of electrons reaching the anode is found using

$$N_e = \frac{N_0 e^{(\alpha-\eta)d}}{1-\frac{\alpha\gamma}{\alpha-\eta}(e^{(\alpha-\eta)d}-1)} \tag{2.7}$$

leading to an approximation of the current through the gap

$$i \approx \frac{i_0 e^{(\alpha-\eta)d}}{1-\frac{\alpha\gamma}{\alpha-\eta}(e^{(\alpha-\eta)d}-1)} \tag{2.8}$$

Townsend breakdown is valid until the number of electrons in the avalanche reaches around 10^8 electrons. In this region, the breakdown changes its behaviour, leading to a new mechanism called streamers.

2.2 Streamer mechanism

At ion concentrations higher than 10^8 in air, Raether (Raether 1964) found that the growth of the electron avalanche increased rapidly. At this ion concentration, the space charge field at the head of the avalanche becomes high enough to distort the applied field and generate self-propagating electron avalanches, increasing the avalanche growth. This may lead to development of plasma channels called streamers. From Kuffel (E. Kuffel, Zaegel, and J. Kuffel 2000), these streamers are characterised by shorter time lags and more rapid breakdowns than what is observed for Townsend mechanism.

The transition from avalanche to streamer happens when the gap length, d, is larger than a critical length, x_c, of the avalanche path in the field direction, leading to an avalanche charge equal to the critical charge. The critical length is determined by the effective ionisation coefficient per unit length, $\overline{\alpha}$, and the total number of electrons needed for streamer inception, N_{cr}. This leads to the streamer criterion for spark formation

$$\int_0^{d \geq x_c} \overline{\alpha} \mathrm{d}x = \ln N_{cr} \tag{2.9}$$

The streamer criterion can be used to iteratively calculate the streamer inception voltage by integrating the effective ionisation coefficient along the electrical field lines and scaling the field until equality is attained for a specific N_{cr}.

The effective ionisation coefficient used in Eq. 2.9 depends on the type of gas, electrical field strength, and pressure. For technical air, $\overline{\alpha}$ can be calculated using the following relationships

$$\frac{\overline{\alpha}}{p} = 1.6053 \cdot \left[\frac{E}{p} - 2.165\right]^2 - 0.2873 \quad (\text{mm·bar})^{-1}, \quad \text{if} \quad 2.588 \leq E/p < 7.943 \ \frac{\text{kV}}{(\text{mm·bar})} \tag{2.10}$$

$$\frac{\overline{\alpha}}{p} = 16.7766 \cdot \frac{E}{p} - 80.006 \quad (\text{mm·bar})^{-1}, \quad \text{if} \quad E/p \geq 7.943 \ \frac{\text{kV}}{(\text{mm·bar})} \tag{2.11}$$

where E is the incremental electrical field size in kV/mm over a small distance Δx, and p is the pressure in bar (Zaengl and Petcharaks 1994).

2.2.1 Time lag

When the peak voltage, V_p, is higher than the lowest breakdown voltage, the static voltage V_s, there is a chance that the impulse leads to a breakdown (E. Kuffel, Zaegel, and J. Kuffel 2000). This statistical virtue of short-front voltage breakdowns is highlighted in the time lag, t, defined as the time from when the voltage $V(t)$ exceeds V_s until a breakdown occurs. The time lag consists of the statistical time lag, t_s, and the formative time lag, t_f. The statistical time lag is the time for a primary electron to appear, and is dependent on the preionisation of the gap. The preionisation is further dependent on the gap distance and radiation producing primary electrons. The formative time lag is the time from primary electrons appearing to a breakdown is developed. The time lags are shown in Fig. 2.1 for a standard lightning impulse.

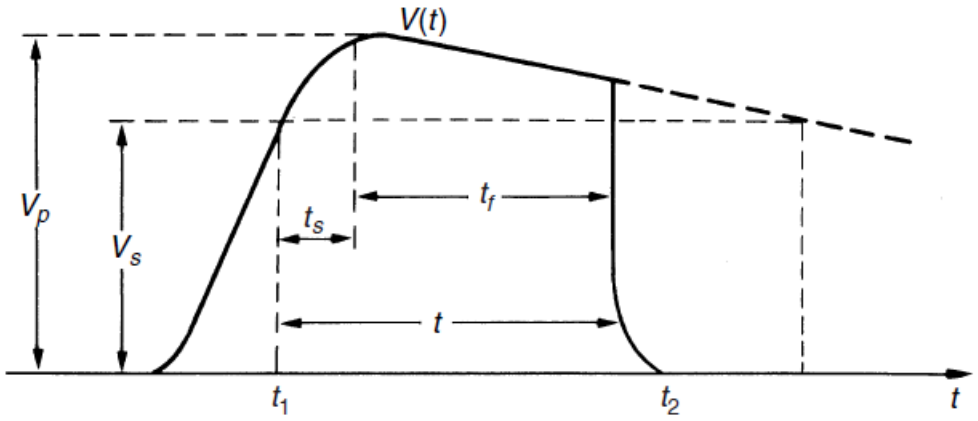

Figure 2.1: The time lags t, t_s, and t_f for a standard lightning impulse with breakdown (E. Kuffel, Zaegel, and J. Kuffel 2000).

2.2.2 Streamer inception

Streamers can be placed into three categories as shown in Fig. 2.2 depending on the inhomogeneity of the gap. The figure shows the expected breakdown voltage for a sphere-sphere gap (red line) and a rod-plane gap (dotted line) when the gap distance and correspondingly the inhomogeneity is increased. The streamer inception "area" in Fig. 2.2 is the voltage and distance at which streamer inception immediately leads to breakdown for a homogeneous electrical field. The streamer inception criterion from Eq. 2.9 can then be used to find the flashover voltage for low probability of breakdown (Pedersen, Blaszczyk, and Boehme 2009).

2.2.3 Streamer propagation

In inhomogeneous electrical fields such as for a rod-plane gap (dotted line in Fig. 2.2), the field strength at the end of the streamer path is not sufficient for a streamer to propagate. In addition to the streamer criterion, a sufficient voltage must be applied for the streamer to propagate to the counter electrode. This voltage can be found using

$$U_{sp} = U_0 + d \cdot E_{st} \tag{2.12}$$

where U_{sp} is the lowest voltage which enables streamer propagation, U_0 is the potential of the streamer head, d is the electrode spacing, and E_{st} is the internal field strength along the streamer. E_{st} is also the necessary external field for stable streamer propagation (Pedersen, Blaszczyk, and Boehme 2009).

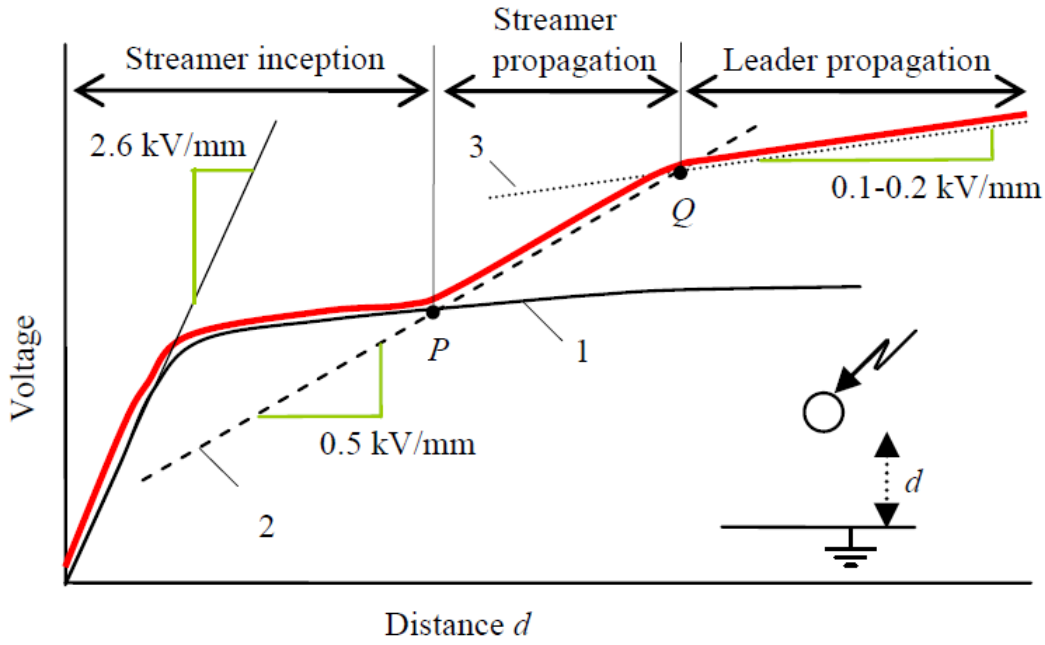

Figure 2.2: Streamer inception and propagation in atmospheric air at 1 bar for a sphere-plane geometry (red line). Point P is the transition from weakly to strongly inhomogeneous field. The dashed line represents a rod-plane geometry (Pedersen, Blaszczyk, and Boehme 2009).

2.3 Up-and-down method

For a normal distributed breakdown voltage, a statistical approach is necessary to estimate the 50% breakdown voltage, $U_{50\%}$, and the standard deviation, σ. Such methods could be the constant-voltage test, the rising-voltage test, or the up-and-down method. The last method, originally proposed by Dixon and Mood (Wolfgang Hauschild and Wolfgang Mosch 1992), provides a reliable method for estimating $U_{50\%}$ and σ in a time-efficient manner. It is based on choosing a fixed voltage amplitude ΔU and an initial voltage U_{00} with certainty of no breakdown. The voltage is first increased by ΔU for each impulse until the first breakdown occurs. Afterwards, the voltage is further increased by ΔU if no breakdown occurs, or decreased by ΔU if a breakdown occurs. An example of the up-and-down method for a series of 31 impulse applications is shown in Fig. 2.3. The benefit of this method is the accession of step-voltage in the estimation of $U_{50\%}$ and s. Adjusting the step-voltage will influence the first breakdown voltage and the subsequent probability. The up-and-down method is repeated n times, depending on the tolerated uncertainty of the $U_{50\%}$ estimation. The results are sorted by magnitude and type of event. $U_{50\%}$ is then estimated using

$$U_{50\%} = U_0 + \Delta U \left(\frac{A}{k} \pm \frac{1}{2} \right) \tag{2.13}$$

where k is the sum of least frequent event, $A = \sum_{i=1}^{r} i k_i$, and k_i is the number of events for the ith voltage step. U_0 denotes the lowest voltage of the rarest event. The sign in Eq. (2.13) is negative if breakdowns are the rarest event and positive if non-breakdowns are the rarest event. Dixon and

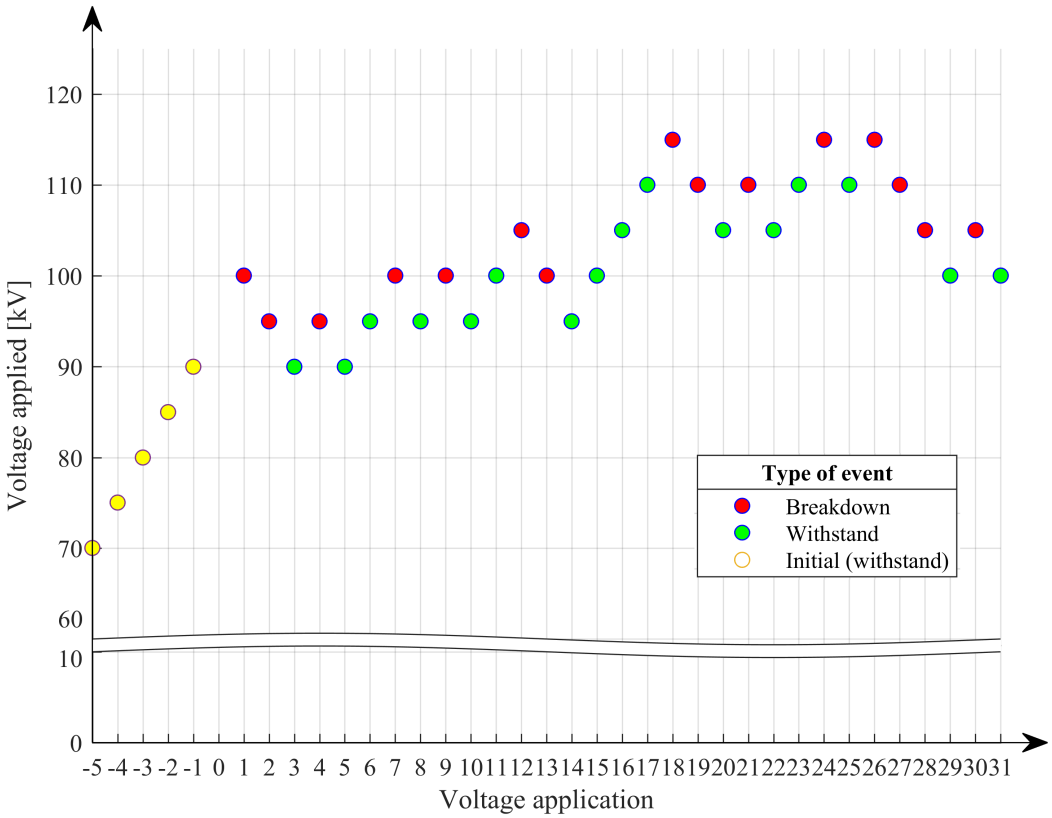

Figure 2.3: A reference series demonstrating the up-and-down method with a step voltage of 5 kV and 31 voltage applications.

Mood also introduced a method to find an estimate, s, of the standard deviation using

$$s = 1.62 \cdot \Delta U \left(\frac{kB - A^2}{k^2} + 0.029 \right) \tag{2.14}$$

where $B = \sum_{i=1}^{r} i^2 k_i$ (Wolfgang Hauschild and Wolfgang Mosch 1992).

The uncertainty of $U_{50\%}$ can also be estimated using

$$s_m = G \frac{s}{\sqrt{k}} \tag{2.15}$$

where G is a factor for standard error found in the published work of Dixon and Mood using the relationship ΔU divided by either σ or the estimated value s (Dixon and Mood 1948).

By using the standard normal distribution, it is also possible to calculate the value, x, at which the outcome is determined by given percentage for a known mean, μ, and standard deviation, σ, without measuring the voltage using the extended up-and-down method. This value is found using

$$x = \sigma z + \mu \tag{2.16}$$

where z is the value corresponding to the tabular value from the standard normal distribution corresponding to a specified probability (Walpole et al. 2012).

2.4 Insulation coordination

Breakdowns from lightning impulses in self-restoring gases has previously been shown to require statistical representation. When finding the correct maximum system voltage, the statistical basic lightning impulse insulation level (BIL) is a useful value. IEEE std 1427 defines this value as the crest value at which 10% of impulses result in breakdown (White 2007). Using this value, the recommended maximum system value can be found. The statistical BIL can be found by using $U_{50\%}$ as an estimate for μ and s as an estimate for σ in Eq. 2.16 together with the appropriate tabular value from the standard normal distribution corresponding to the BIL probability.

2.5 Inhomogeneity factor

Fig. 2.2 shows the importance of field inhomogeneity for streamers. In a homogeneous field, the streamer criterion from Eq. 2.9 immediately leads to a breakdown, while for more inhomogeneous fields, an additional potential is necessary after transitioning from the streamer inception area. To analyse streamer inception, field lines and the inhomogeneity factor are therefore important tools. In the numerical analysis, the inhomogeneity factor is defined as

$$\eta = \frac{E_{max}}{E_{avg}} = \frac{E_{max} l_{ag}}{U} \tag{2.17}$$

where E_{max} is the maximum field strength along the critical path, E_{avg} is the average field strength along the critical path, l_{ag} is the length of the critical path and U is the terminal voltage.

3 Method

The purpose of the project is to outline some of the dielectric properties of AirPlus and synthetic air. A standard lightning impulse (Fig. 3.1) is used to determine the breakdown characteristics using the up-and-down method, estimating $U_{50\%}$ and the standard deviation. Both AirPlus and synthetic air will be stressed with positive and negative lightning impulses to investigate a potential difference in breakdown voltage between the two polarities. The gases are also analysed for both 1.00 bar and 1.50 bar pressure with 1-1.3 bar being normal for GIS utilising SF_6 in distribution and industry mediums in the lower range of medium-voltage (Kaveh Niayesh and Magne Runde 2017). Finally, the gap distance will be adjusted from 10 mm up to a maximum of 80 mm. The gap distance will be limited by the maximum peak voltage of 150 kV set by the insulation of the conductor entry-point to the test tank.

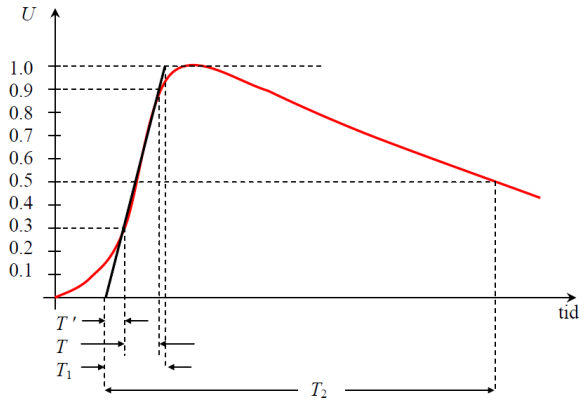

Figure 3.1: Standard lightning impulse with a front time (T_1) of 1.2μs and time to half value (T_2) of 50 μs (Høidalen 2016).

Four electrodes have been chosen in combination with a grounded plane-type electrode. The dimensions are shown in Fig. 3.2. Three rods with hemispherical ends of varying radius will represent inhomogeneous field distribution in rod-plane gaps, and the plane-plane gap will represent a quasi-homogeneous field distribution. The non-uniformity values for the configurations can be found in Appendix C.

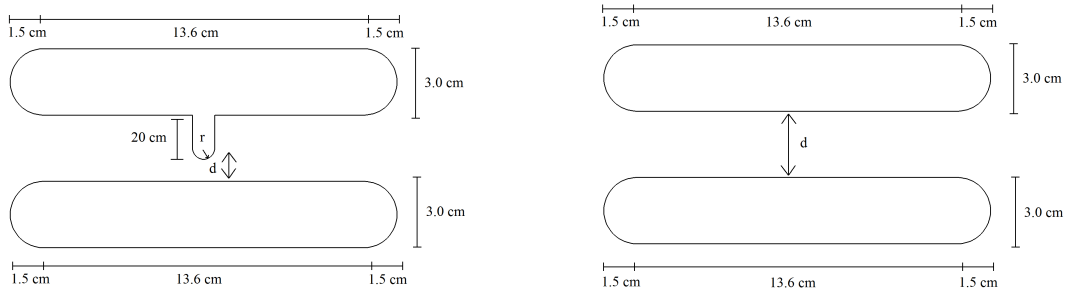

(a) The rod-plane configuration

(b) The plane-plane configuration

Figure 3.2: Electrode set-ups used. The variable r represents the radius for the three different rods and d is the gap length.

The estimation of 50% breakdown voltage and standard deviation will be based on the up-and-

down method by Dixon and Mood. The step voltage should be chosen as close to the standard deviation as possible. This could only be done by making an educated guess with knowledge from previous results. The suggested limits for the step voltage are between 0.5σ and 2.0σ (Dixon and Mood 1948). The number of repetitions for each up-and-down series has been chosen to be 31 due to time constraint. If chosen too low, a high standard deviation is to be expected. The chosen value is deemed high enough to yield acceptable results as the rate of improvement in estimation is greatly reduced beyond this number of voltage applications (Wolfgang Hauschild and Wolfgang Mosch 1992). Each voltage application is separated by 1 minute to achieve independence between the results.

The peak voltage of each impulse is measured together with the type of event (breakdown or withstand). The values are used in Eqs. 2.13 and 2.14 to estimate the 50% breakdown voltage and standard deviation respectively. The voltage used in Eq. 2.13 is the impulse generator output voltage, not the measured impulse voltage as this value does not persistently change with ΔU. In addition, the temperature, pressure and density are recorded to investigate potential deviations. No correction method for $U_{50\%}$ in AirPlus has yet been found.

3.1 Experimental set-up

The circuit used in the experiments is shown in Fig. 3.3. The impulse generator is a High Volt IP 60/1200 L Impulse voltage generator rated at 1.2 MV. The minimum step voltage can be adjusted depending on the chosen maximum set-up voltage (0.1 kV for each 100 kV interval). The measured voltage is reduced through a capacitive voltage divider to reduce the input voltage to a safe level for the measuring equipment. The maximum impulse voltage is set to 500 kV by using 5 of the 12 available levels whenever possible to achieve a satisfactory front time for the lightning impulse. IEC 60060-1:2010 limits the deviation from $1.2\mu s$ to ± 30% (International Electrotechnical Commission 2010).

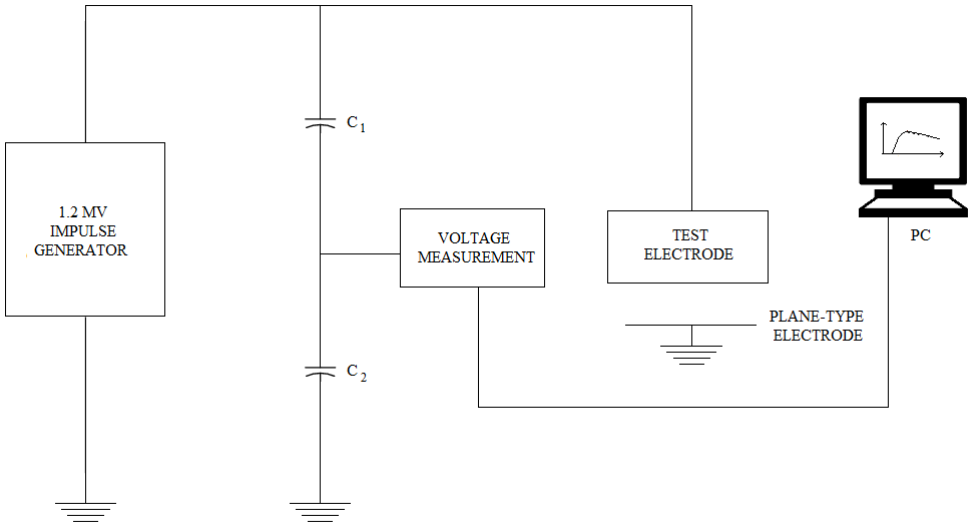

Figure 3.3: Circuit diagram of the experimental set-up used to stress the electrode gaps with lightning impulses.

The lightning impulse is fed into the gas-sealed tank containing the electrodes. The insulation of the conductor feed-through on top of the tank limits the maximum impulse voltage to 150 kV, and thus the maximum gap distance between the electrodes.

To change the gap distance inside the sealed tank, a crank is used to adjust the ground electrode from the outside. This crank has the property of adjusting the gap distance with exactly 2 mm for each rotation. This property was used to increase the gap distance in a controlled manner without having to perform measurements inside the tank while it was sealed off.

The electrodes are changed from AirPlus to synthetic air. For AirPlus, the rod electrodes were made of copper, while for synthetic air the rod electrodes were made of brass. For both gases, the grounded plane-type and the top plane-type electrode were both made of aluminium. The difference in rod material is simply a result of an error, but should have minor impact on the final results.

3.2 Experimental procedure

The experimental work had a restriction on both time and amount of C_5 PFK available. AirPlus was therefore only changed when changing electrodes, and measurements for each electrode configurations were therefore performed using the same AirPlus gas.

The electrodes were first cleaned with isopropanol to remove potential surface pollution. The gap was then adjusted to 10 mm using an aluminium cylinder of this exact length. The length was chosen to limit the error where it has the most impact. After adjusting the gap, the tank was then sealed and evacuated to a pressure of <1 mbar. To mix C_5PFK and synthetic air, crating AirPlus, the tank was first filled with C_5PFK to 0.113 bar. This is approximately 7.5 volume-percent for AirPlus at 1.50 bar. After reaching the pressure and a waiting time of at least a minute, synthetic air was mixed into the C_5PFK until a pressure of 1.50 bar is reached. Some minutes of waiting time afterwards were necessary until achieving stable pressure measurement.

All up-and-down series were performed in the same order in AirPlus. The tests in synthetic air was not performed in any systematic order as the results are used as a reference. The gap distance is increasingly adjusted from 10 mm until it is finally brought back to 10 mm for a retest to investigate potential influence on the number of breakdowns on $U_{50\%}$. For each gap length, positive polarity LI is tested before negative LI. After 1.50 bar has been tested, AirPlus is then evacuated and stored in a container until 1.00 bar is reached, and the procedure performed once more for this pressure. The test order of the electrodes in AirPlus were first the 5 mm rod, then the plane-type, thirdly the 10 mm rod, and finally the 2.5 mm rod.

3.3 Gas handling

To empty and fill the tank containing the test objects, the system shown in Fig. 3.4 was used. AirPlus is treated as a polluting gas, and therefore stored (final vacuum <5 mbar) in a separate container after use. The same system is used for technical air, but without storage of used gas. To create the AirPlus volume-concentration of 7.5% C_5 PFK and 92.5% synthetic air, the system is first evacuated to vacuum (<1 mbar) using a B143R11 Dilo service cart. The tank is then filled with C_5 PFK until the pressure reaches 0.113 bar. It is further filled with synthetic air until a final pressure of 1.50 bar is reached. For

experiments at 1.00 bar, AirPlus is removed from the 1.50 bar filling until a final pressure of 1.00 bar is reached. The tank is only filled with AirPlus once for each electrode configuration. Gas analysis was performed for the last tested configuration, the 10 mm rod electrode, at 1.50 bar by using two small containers with vacuum connected to the top of the tank to investigate potential influence of by-products created by the electrical breakdowns. 1.50 bar was chosen due to equipment restrictions with over-pressure necessary for the analysis to be performed, even though AirPlus at 1.00 bar would have been exposed to more breakdowns.

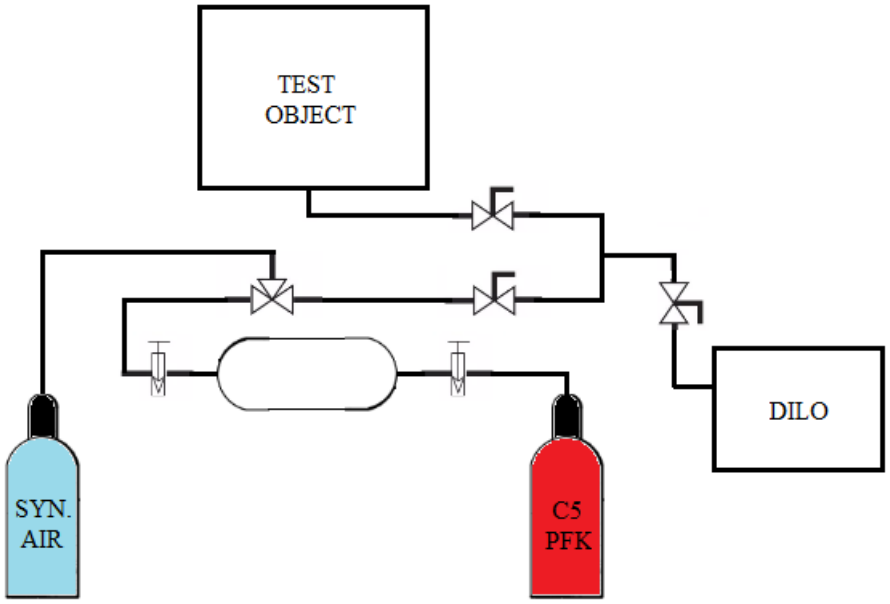

Figure 3.4: Gas handling system used for filling and emptying the tank (test object) containing the electrode configuration.

3.4 Numerical analysis

The streamer inception voltage can be found for homogeneous gaps by using the streamer criterion from Eq. 2.9 iteratively if the ionisation coefficient and the stability charge are known. The theoretical streamer inception voltage is found by calculating the ionisation coefficient for a small iteration along the electrical field lines and summing all steps. If this value is lower than the streamer criterion, the voltage is increased by an increment, and the process repeated. The geometries are quite simple, and analytic formulas can be used to find the field distributions.

The most important region in the model for rod-plane is the field line starting at the tip of the rod with the shortest path to ground. The COMSOL Multiphysics model for rod-plane is therefore highly focused on this region. For the plane-plane configuration, the maximum field strength is located on the edges, meaning that the edges become quite important. The scope is therefore highly increased to include the true size of the tank.

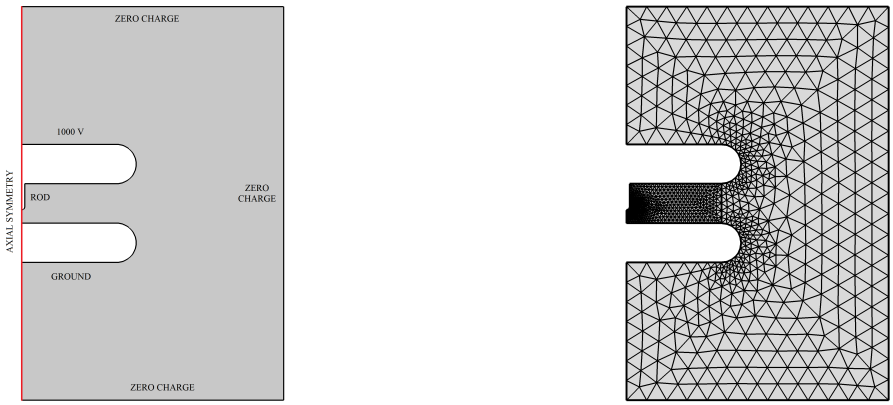

(a) Geometry and physics

(b) Mesh resolution

Figure 3.5: COMSOL Multiphysics model for numerical analysis of the rod-plane configurations.

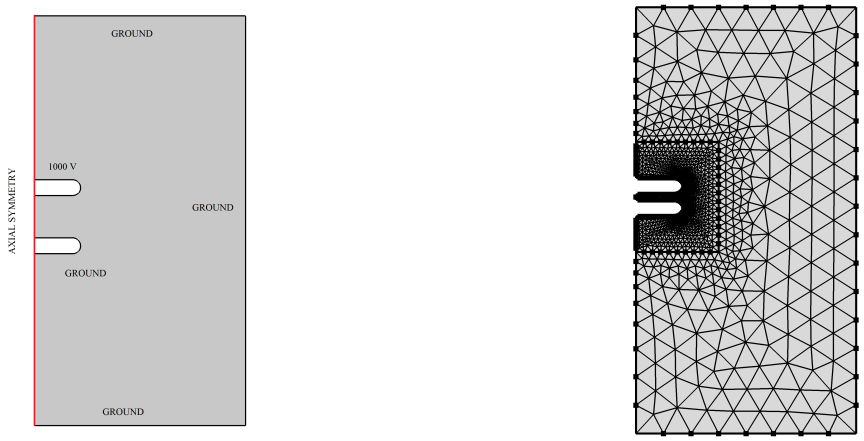

(a) Geometry and physics

(b) Mesh resolution

Figure 3.6: COMSOL Multiphysics model for numerical analysis of the plane-plane configuration.

4 Results

The following section presents the measured results from the up-and-down method by Dixon and Mood for both synthetic air and the new AirPlus insulation gas. The dependency of gap length on $U_{50\%}$ will first be explored to investigate the difference in withstand capabilities of the two gases. Potential differences in LI polarity in AirPlus will also be investigated. The impact of inhomogeneity factor on both gases will further be explored.

The set-ups used are shown in Fig. 3.2b for plane-plane and Fig. 3.2a for the three rod-plane configurations. The radius used to differentiate the three rod electrodes denotes the radius of the hemispherical end pointing towards the grounded plane-type electrode.

The most essential numerical results for the laboratory results can be found in Appendix A.

4.1 Dependency on gap distance, polarity, and pressure

The first subsection investigates the impact of gap distance for the various electrode configurations on both insulation gases. The expected theoretical characteristics are found in Fig. 2.2 for synthetic air. Most of the results for the rod-plane configuration are below the limit for streamer propagation (40-50 mm) (Pedersen, Blaszczyk, and Boehme 2009), and a constant stability field, E_{st}, across the different electrodes are therefore not expected for synthetic air.

4.1.1 Synthetic air

Plane-plane

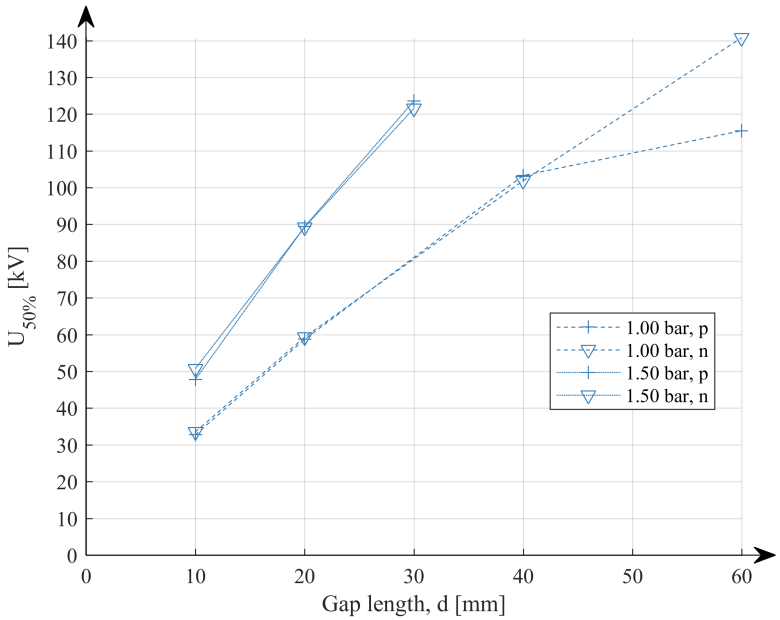

Figure 4.1: $U_{50\%}$ as a function of gap length for the plane-type electrode in synthetic air.

The homogeneous field distribution created by the plane-plane gap should result in a negligible difference between the polarity of the applied LI. The results in Fig. 4.1 shows the consistency be-

tween theory and measurements for all but one series. The positive polarity series at 1.00 bar and 60 mm gap is lower than the negative impulse series at the same pressure and gap length. From 40 mm to 60 mm the inhomogeneity factor from Table C.1 increases from 1.6 to 2.1, a change large enough that could explain the sudden deviation in $U_{50\%}$ between negative and positive polarity. For more inhomogeneous fields, positive polarity LI are expected to result in a lower $U_{50\%}$ than negative LI.

The internal field strength, i.e. the slope of $U_{50\%}$ from Eq. 2.12, is 2.1 kV/mm at 1.00 bar and approximately 3.6 kV/mm for 1.50 bar. The expected value for the field strength air is approximately 3.9 $\mathrm{kVmm^{-1}bar^{-1}}$ (i.e. 2.6 $\mathrm{kVmm^{-1}}$ at 1.00 bar and 4.7 $\mathrm{kVmm^{-1}}$ at 1.50 bar) in a truly homogeneous field as the field strength is expected to increase proportional with pressure (E. Kuffel, Zaegel, and J. Kuffel 2000). The linear curve should originate in origo, yet the offset is over 10 kV for both, most likely caused by a low variation in gap distance leading to poor extrapolation in the streamer inception area of the curve in Fig. 2.2. This offset, as well as an increasingly inhomogeneous field, transitioning towards streamer propagation, could explain the lower measured internal field strength than expected.

Table 4.1: Linear regression analysis of plane-plane results in synthetic air

Pressure [bar]	Polarity	E_{st} [kV/mm]	U_0 [kV]	R^2
1.00	+	1.7	22.9	0.93
1.00	-	2.1	14.7	1.00
1.50	+	3.8	11.1	1.00
1.50	-	3.5	16.4	1.00

Rod-plane, 10 mm radius

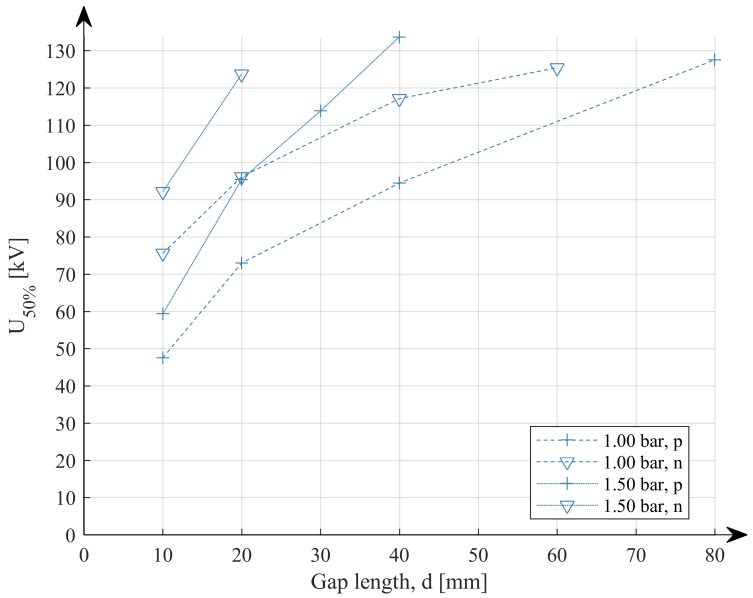

Figure 4.2: $U_{50\%}$ as a function of gap length for the 10 mm radius rod electrode in synthetic air.

For the rod with the largest hemispherical radius, the measured critical flashover voltage in Fig. 4.2 illustrates the characteristics of breakdowns in synthetic air. $U_{50\%}$ increases with the gap length for each iteration, which is expected as the ionisation coefficient is dependent on the electrical field. The electrical field is further dependent on gap length, reducing the field strength for increasing gap distance. For the rod-plane configuration, polarity also becomes important. In air, positive LIs should have a lower internal field strength needed for propagation than negative LIs, and therefore a lower withstand voltage (Pedersen, Blaszczyk, and Boehme 2009). $U_{50\%}$ should therefore be lower for positive LI. The measurements in Fig. 4.2 illustrates this behaviour quite well. All positive LI at equal pressure results in a lower $U_{50\%}$ than negative LI. Thirdly, the values for 1.00 bar should be lower than for 1.50 bar as the mean free path of the electrons, which is inversely proportional to the pressure, will affect the probability of ionising electron collisions (E. Kuffel, Zaegel, and J. Kuffel 2000).

The results from linear regression of the curves in Fig. 4.2 are shown in Table 4.2. The estimated E_{st} for 1.00 bar and positive LI indicates that the streamer created has not yet entered the linear region of streamer propagation as the value is twice that of the theoretical value.

Table 4.2: Linear regression analysis of results for the 10 mm rod in synthetic air

Pressure [bar]	Polarity	E_{st} [kV/mm]	U_0 [kV]	R^2
1.00	+	1.1	45.5	0.95
1.00	-	1.0	72.2	0.92
1.50	+	2.4	40.2	0.97
1.50	-	3.2	60.5	1.00

Rod-plane, 5 mm radius

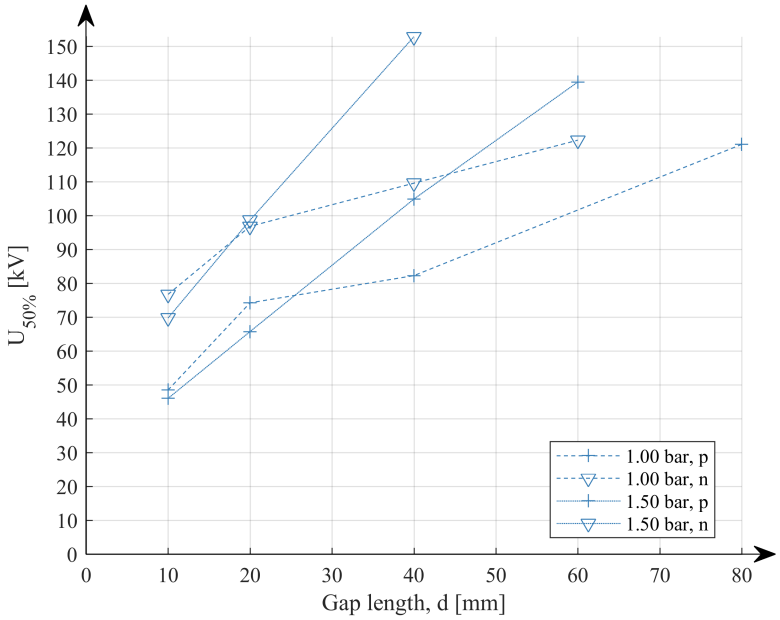

Figure 4.3: $U_{50\%}$ as a function of gap length for the 5 mm radius rod electrode in synthetic air.

The results for the 5 mm hemispherical rod in Fig. 4.3 for synthetic air has a divide between results for the lowest gap lengths and the largest gap lengths. For the largest gap lengths (≥40 mm), $U_{50\%}$ holds the characteristics one would expect. The voltage increases with both gap distance and pressure. Negative polarity LI has a higher withstand capability than positive LI.

For the shortest gap lengths (<40 mm), $U_{50\%}$ starts to behave unexpectedly. The voltage still increases with gap lengths, and the positive polarity LI is the most important, but the voltage decreases with increasing pressure where both polarities result in higher $U_{50\%}$ at 1.00 bar than at 1.50 bar. The estimated uncertainty of $U_{50\%}$ is not large enough to explain these deviations.

For 1.00 bar, the inception field found in Table 4.3 is much lower than for 1.50. The streamer potential is higher for both series with negative LI compared to positive LI at the same pressure.

Table 4.3: Linear regression analysis of results for the 5 mm rod in synthetic air

Pressure [bar]	Polarity	E_{st} [kV/mm]	U_0 [kV]	R^2
1.00	+	0.9	46.1	0.95
1.00	-	0.9	73.8	0.93
1.50	+	1.9	28.1	1.00
1.50	-	2.8	42.7	1.00

Rod-plane, 2.5 mm radius

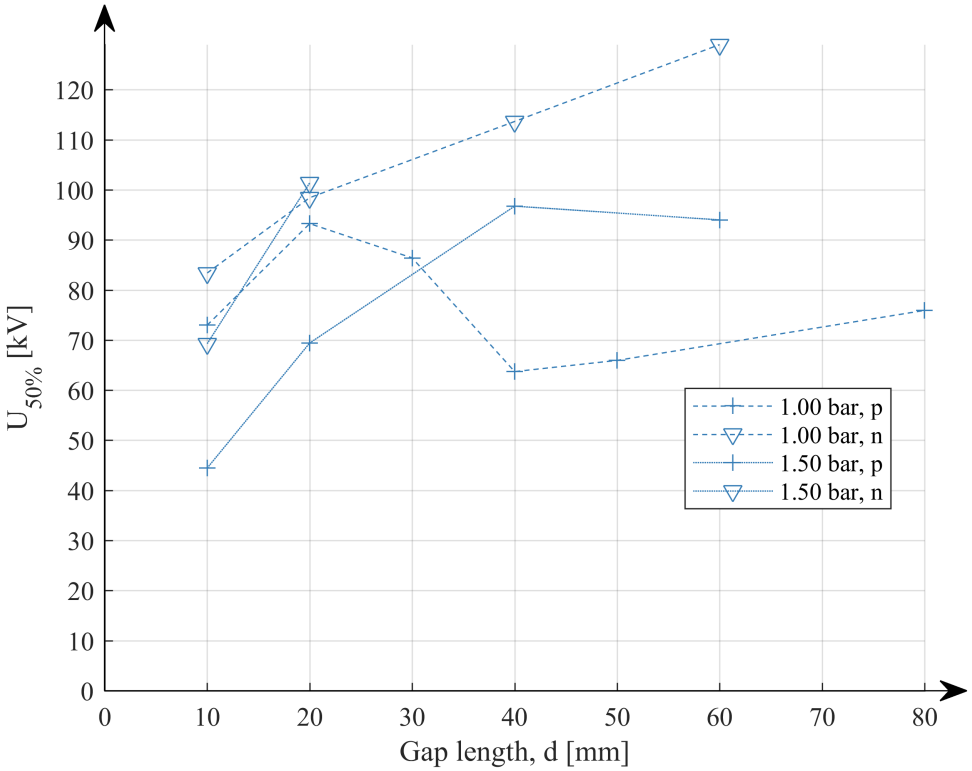

Figure 4.4: $U_{50\%}$ as a function of gap length for the 2.5 mm radius rod electrode in synthetic air.

The measured $U_{50\%}$ in Fig 4.4 for the smallest electrode behaves contrary to theoretical expectations. For small gap lengths, the positive LI voltage for 1.00 bar is much higher than for 1.50 bar (almost 60% higher at the maximum), the opposite of what one would expect. The same is true for negative LI for 10 mm gap length. Approaching 40 mm gap length and beyond, the critical flashover voltage is restored to more normal behaviour. The strange behaviour of $U_{50\%}$ is reflected in Table 4.4 where the inception field is negative, although with a very poor linear fit. A thorough discussion on possible causes can be found in Section 4.6.

Table 4.4: Linear regression analysis of results for the 2.5 mm rod in synthetic air

Pressure [bar]	Polarity	E_{st} [kV/mm]	U_0 [kV]	R^2
1.00	+	-0.2	82.1	0.10
1.00	-	0.9	77.6	0.98
1.50	+	1.0	44.4	0.79
1.50	-	3.2	37.2	1.00

4.1.2 AirPlus

Plane-plane

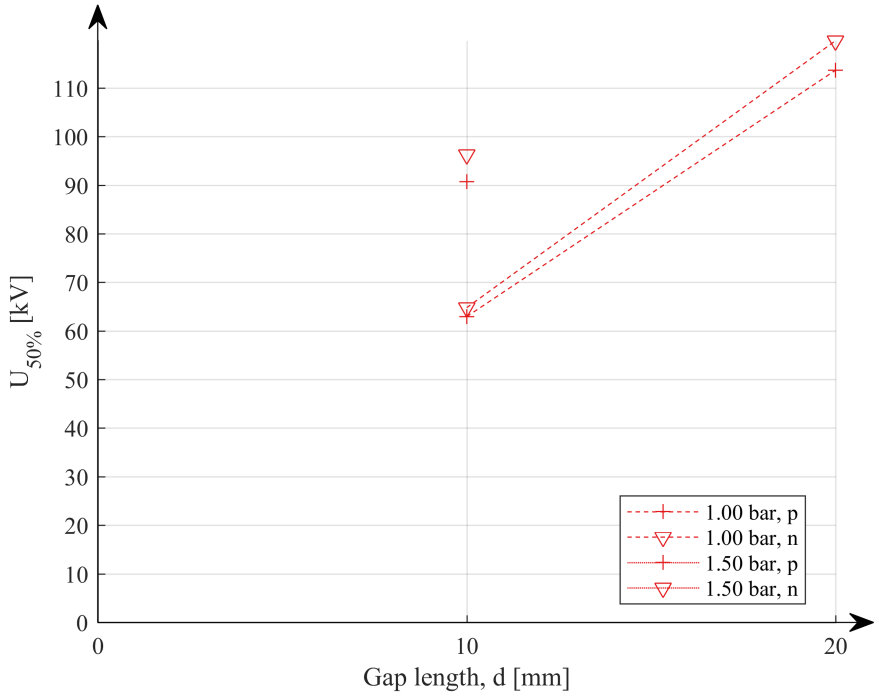

Figure 4.5: $U_{50\%}$ as a function of gap length for the plane-type electrode in AirPlus.

The results in Fig. 4.5 show that the polarity of the LI is of little importance in a homogeneous field distribution in AirPlus, although the estimated $U_{50\%}$ is not a perfect match for all results. The negative LI generates a higher $U_{50\%}$ (less than 5%) than for positive LI. This is the opposite of what is observed for the other configurations. The estimated uncertainty of $U_{50\%}$ is not large enough to neglect the difference.

The internal field strength for AirPlus is estimated to approximately 5.3 kVmm^{-1} at 1.00 bar. Only two measurements series for this pressure level makes the estimate of the inception field quite inaccurate, while for 1.50 it is impossible to make even a rough estimate due to the high dielectric strength preventing further variation in gap distance. For an AirPlus mixture of 10.4% C_5 PFK and 89.6% technical air (molar fractions), Saxegaard et. al. estimated the inception field to be 4.3 kVmm^{-1}bar^{-1} (Magne Saxegaard et al. 2018).

Table 4.5: Linear regression analysis of plane-plane results in AirPlus

Pressure [bar]	Polarity	E_{st} [kV/mm]	U_0 [kV]	R^2
1.00	+	5.1	12.2	1.00
1.00	-	5.5	9.90	1.00
1.50	+			
1.50	-			

Rod-plane, 10 mm radius

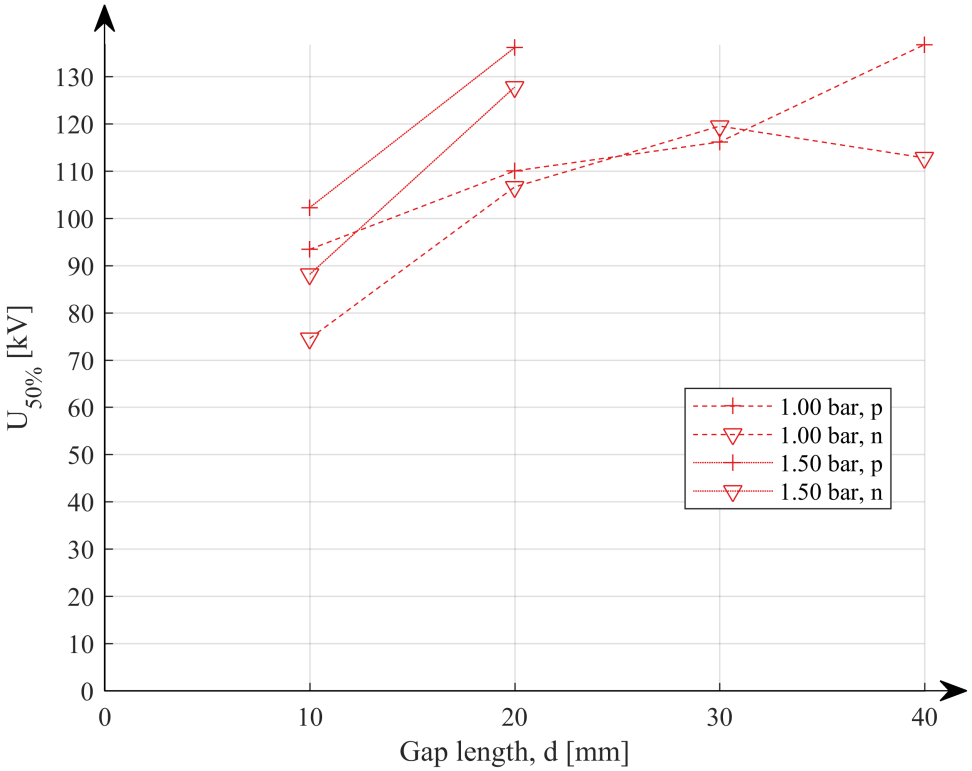

Figure 4.6: $U_{50\%}$ as a function of gap length for the 10 mm radius rod electrode in AirPlus.

The results in Fig. 4.6 for the largest rod in AirPlus do not unquestionably outline the influence of polarity on $U_{50\%}$, but it gives a strong indication that negative polarity is more important than positive polarity for breakdown analysis. In all gap lengths at both pressures, only one has a higher measured $U_{50\%}$ for positive polarity than for negative polarity. The electrode configuration also behaves as expected regarding pressure. All measured $U_{50\%}$ at 1.50 bar are higher than at 1.00 bar.

Regression analysis presented in Table 4.6 show that the inception field is almost three times higher for 1.50 bar than for 1.00 bar. Using the results with an acceptable R^2, i.e. discarding 1.00 bar with negative polarity with an R^2 value of only 0.68, the required potential is higher for positive polarity than for negative polarity.

Table 4.6: Linear regression analysis of results for the 10 mm rod in AirPlus

Pressure [bar]	Polarity	E_{st} [kV/mm]	U_0 [kV]	R^2
1.00	+	1.4	80.0	0.96
1.00	-	1.3	71.5	0.68
1.50	+	3.4	68.4	1.00
1.50	-	4.0	48.5	1.00

Rod-plane, 5 mm radius

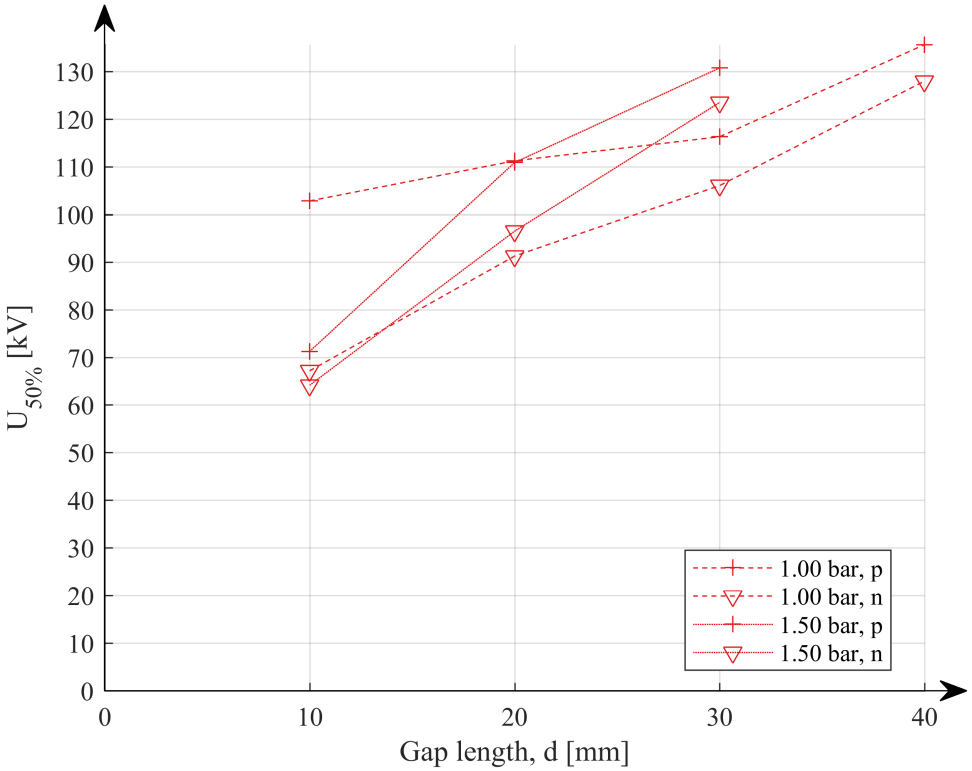

Figure 4.7: $U_{50\%}$ as a function of gap length for the 5 mm radius rod electrode in AirPlus.

In AirPlus, the 5 mm rod in gave results in Fig. 4.7 that are in diagreement with theoretical expectations. For the two longest gaps, the estimated $U_{50\%}$ are higher for 1.50 bar than for 1.00 bar. For the two smallest gaps, the behaviour is not as expected from theory. Positive polarity at 1.00 bar is now equally or even much better than at 1.50 bar. Despite the unexpected results in Fig. 4.7, this rod, as for the largest rod in Fig. 4.6, indicates that negative polarity is more important for breakdown analysis than positive polarity in AirPlus.

The values found in Table 4.7 show that the inception field is higher for 1.50 bar, and positive polarity LIs have lower streamer potential required for breakdown.

Table 4.7: Linear regression analysis of results for the 5 mm rod in AirPlus

Pressure [bar]	Polarity	E_{st} [kV/mm]	U_0 [kV]	R^2
1.00	+	1.0	90.6	0.92
1.00	-	2.0	48.8	0.99
1.50	+	3.0	44.8	0.96
1.50	-	3.0	35.4	1.00

Rod-plane, 2.5 mm radius

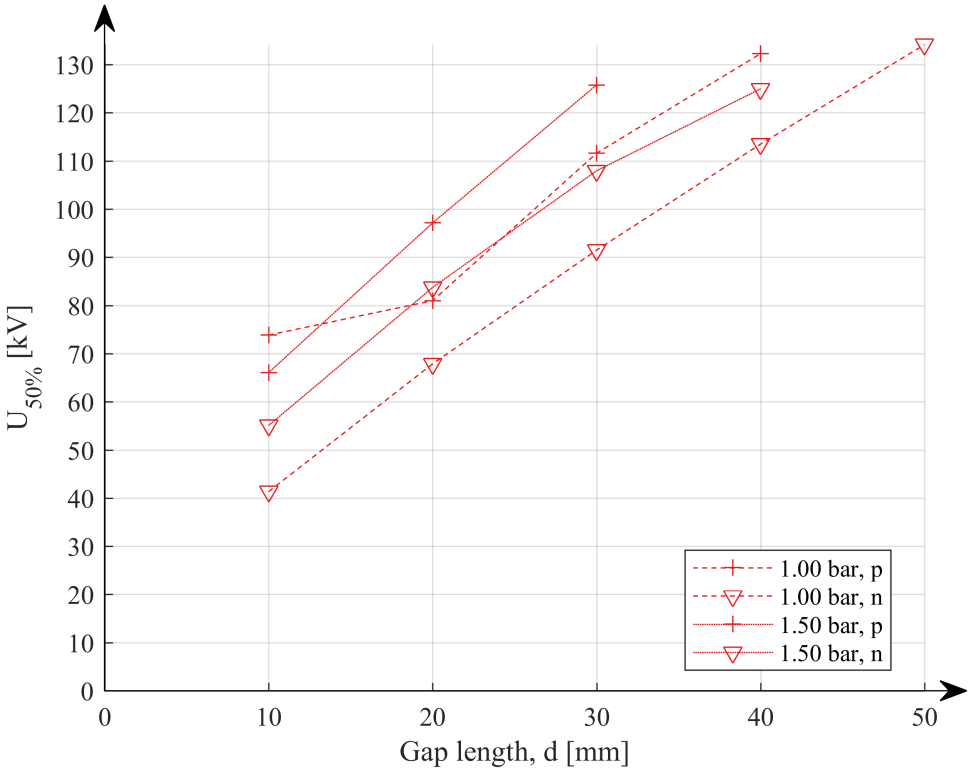

Figure 4.8: $U_{50\%}$ as a function of gap length for the 2.5 mm radius rod electrode in AirPlus.

The smallest rod in AirPlus is more "well-behaved" than the same rod in synthetic air, as can be seen from the measured values for $U_{50\%}$ in Fig. 4.8. For all series, except positive polarity at 10 mm gap, the critical flashover voltage is higher at 1.50 bar than at 1.00 bar. There is also a clear difference in the withstand capability of the two LI polarities. Negative polarity LI is the most critical polarity, with 10-20 kV lower measured $U_{50\%}$ compared with positive LI.

Table 4.8 shows that the streamer potential is higher for positive LIs than for negative LIs. The inception field is also higher for 1.50 bar than for 1.00, as expected.

Table 4.8: Linear regression analysis of results for the 2.5 mm rod in AirPlus

Pressure [bar]	Polarity	E_{st} [kV/mm]	U_0 [kV]	R^2
1.00	+	2.1	48.2	0.95
1.00	-	2.3	20.3	1.00
1.50	+	3.0	36.6	1.00
1.50	-	2.3	34.5	0.99

4.2 Dependency on field distribution, polarity, and pressure

The previous results indicate that inhomogeneity plays a role when comparing the relative performance of both gases. In homogeneous fields, $U_{50\%}$ is greater for AirPlus than for synthetic air, while for more inhomogeneous fields, the relative improvement of AirPlus compared with synthetic air is reduced. The impact of field inhomogeneity will be further investigated in this section by having the shape of the electrodes as the only controllable variable. This implies that the gap length, previously a variable, is now changed to a parameter together with LI polarity and pressure. The only variable is the inhomogeneity of the field, a result of electrode shape variation.

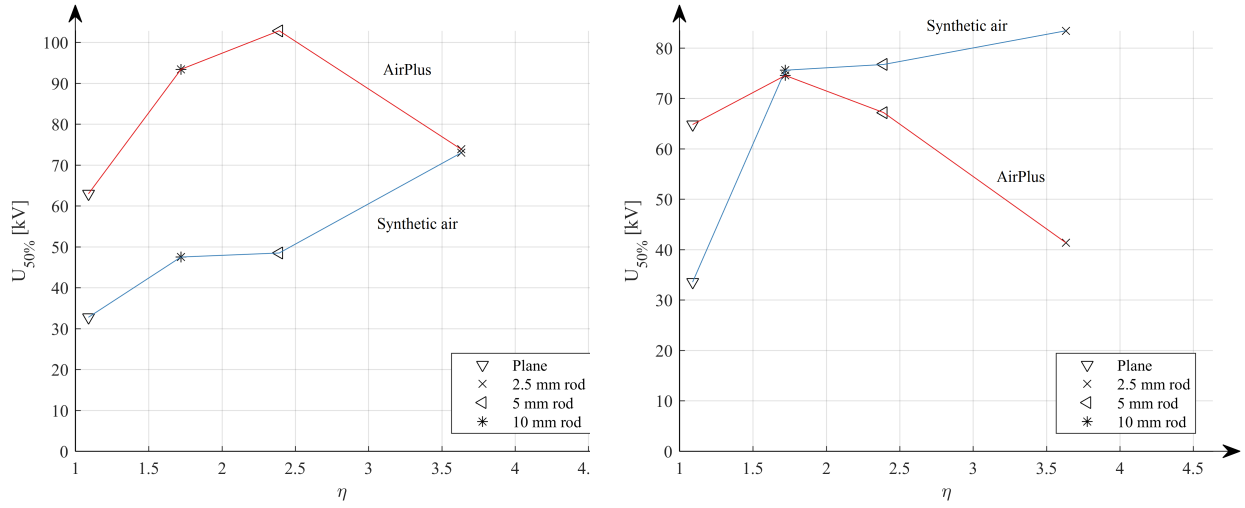

(a) Positive polarity

(b) Negative polarity

Figure 4.9: Effect of inhomogeneity on $U_{50\%}$ in both gases at 1.00 bar and 10 mm gap for the two polarities.

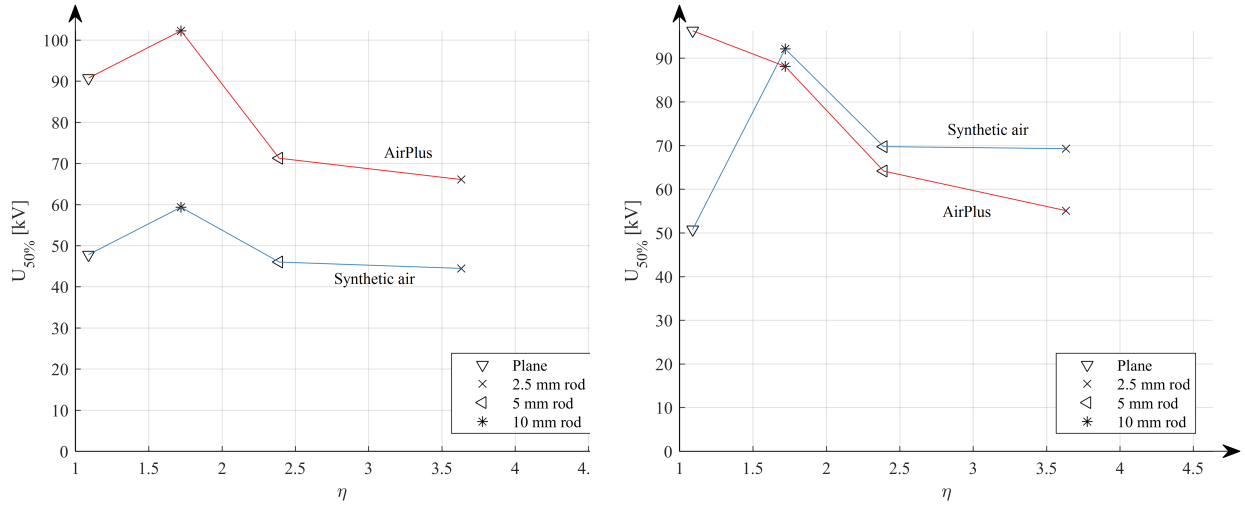

(a) Positive polarity

(b) Negative polarity

Figure 4.10: Effect of inhomogeneity on $U_{50\%}$ in both gases at 1.50 bar and 10 mm gap for the two polarities.

For negative polarity, increasing field inhomogeneity reduces the improvement of AirPlus compared to synthetic air found for homogeneous fields. A decreasing $U_{50\%}$ for increasing η is measured for AirPlus. The same is measured in synthetic air at 1.50 bar, but with an initial rapid increase after changing from plane-plane to the largest rod-plane that results in a higher $U_{50\%}$ for inhomogeneous fields, despite a general decrease in $U_{50\%}$ when reducing the radius of the rod. At 1.00 bar, $U_{50\%}$ is strictly increasing with η, but the results for high inhomogeneity is associated with high uncertainty in synthetic air.

When comparing the results for similar polarity, the distinctive characteristics of AirPlus and synthetic air are evident. At negative polarity, AirPlus performs either comparable to synthetic air, or worse. The exception is of course at quasi-homogeneous fields where polarity should not have an impact on $U_{50\%}$. AirPlus also looks to be more dependent on inhomogeneity at negative polarity. The relative decrease in $U_{50\%}$ for negative LI is substantially larger than for positive polarity. The largest relative decrease for positive LI is a 25% decrease while the smallest relative decrease for negative LI is 37%.

4.3 Comparison of the dielectric performance between synthetic air and AirPlus

There is a strong indication from the results testing $U_{50\%}$ as a function of gap length that negative polarity LIs have lower withstand capabilities than positive LIs in AirPlus. Negative polarity will therefore be used from now on to illustrate the dielectric performance of AirPlus. The same will be done for positive polarity in synthetic air, well known from literature, as they are the limiting factor in insulation coordination respectively.

4.3.1 Plane

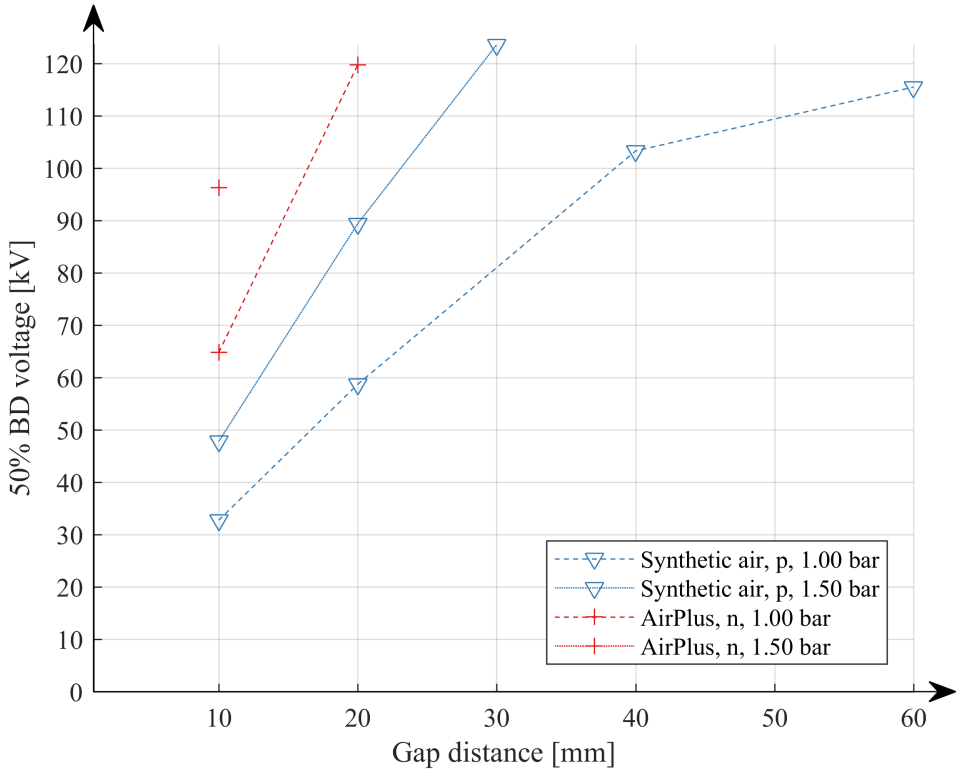

Figure 4.11: Comparison of $U_{50\%}$ as a function of gap length for the plane-type electrode.

The results for homogeneous field show a clear advantage for AirPlus compared with synthetic air. At 10 mm, $U_{50\%}$ for AirPlus is twice the value in synthetic air for both pressures. The excellent performance of AirPlus yielded only three test series in total, as the next increase in gap length resulted in LI voltages surpassing 150 kV. At 1.50 bar, using AirPlus instead of synthetic air could reduce the necessary gap length by 50%, enabling more compact switchgear designs.

4.3.2 10 mm radius

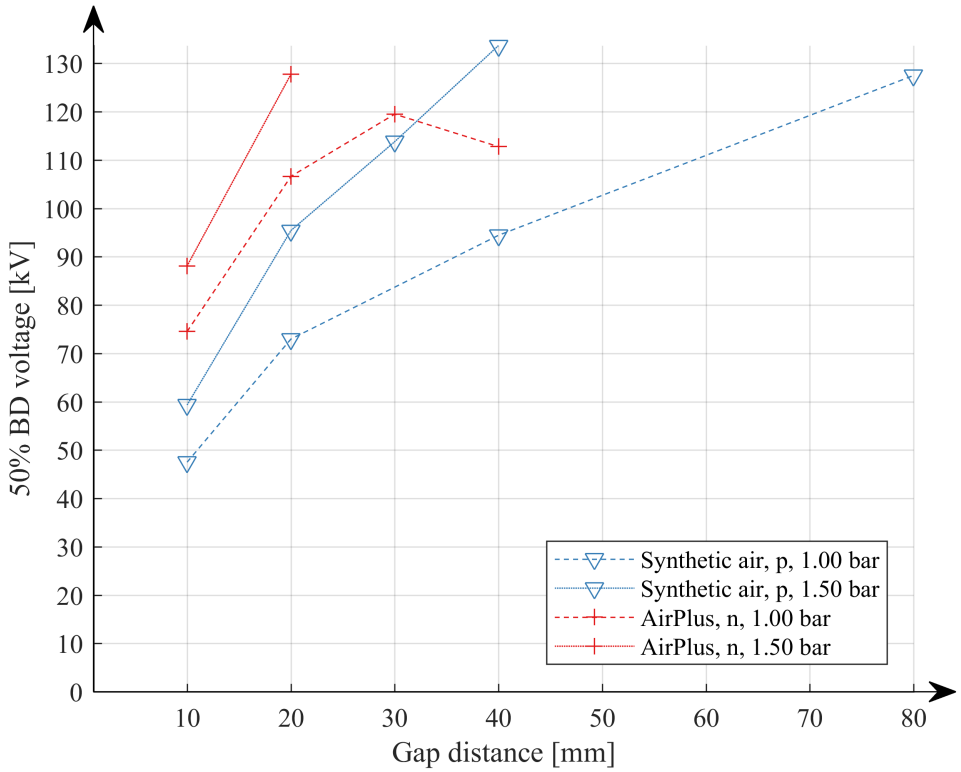

Figure 4.12: Comparison of $U_{50\%}$ as a function of gap length for rod-plane configuration with the 10 mm rod.

The improvement after changing gas from synthetic air to AirPlus is slightly smaller for inhomogeneous fields. At 10 mm, $U_{50\%}$ for AirPlus is only 36% larger at 1.00 bar and 33% at 1.50 bar. The critical flashover voltage at 40 mm in AirPlus could indicate that the inhomogeneity of the gap reduces the withstand capabilities more than it increases due to gap distance, but the standard deviation of this value is quite high (Table A.6). The standard deviation of the estimated $U_{50\%}$ is 10.6 kV.

4.3.3 5 mm radius

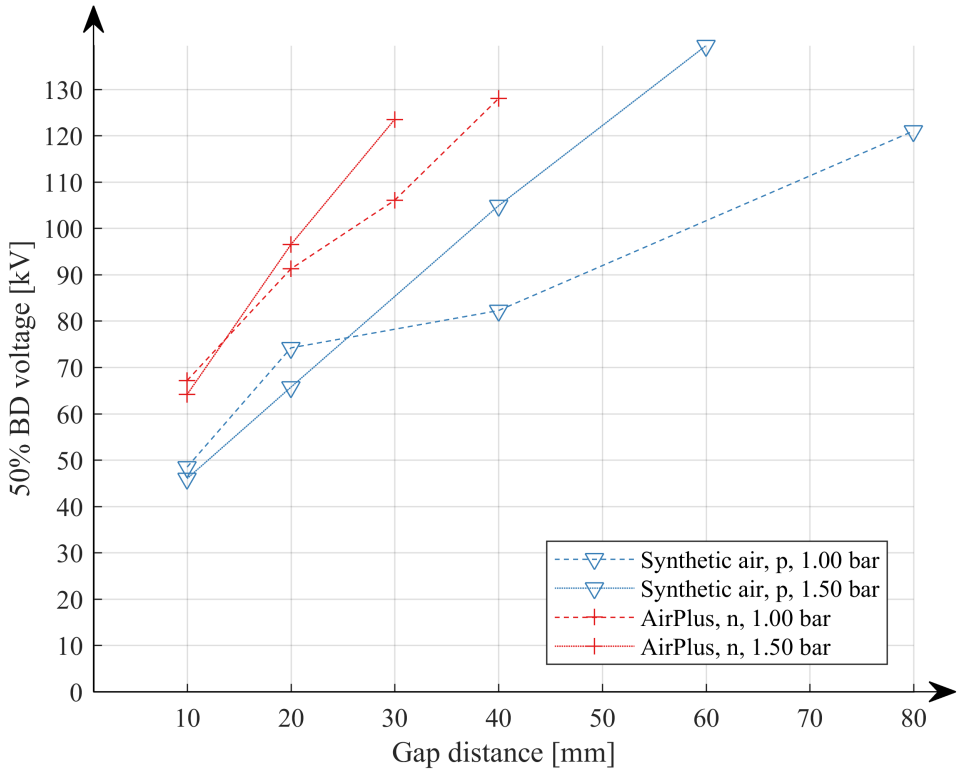

Figure 4.13: Comparison of $U_{50\%}$ as a function of gap length for rod-plane configuration with the 5 mm rod.

Fig. 4.13 further illustrates the reduced relative improvement from synthetic air to AirPlus in more inhomogeneous fields. For 10 mm and 20 mm gap length, both synthetic air and AirPlus have the same rate of increase for $U_{50\%}$.

4.3.4 2.5 mm radius

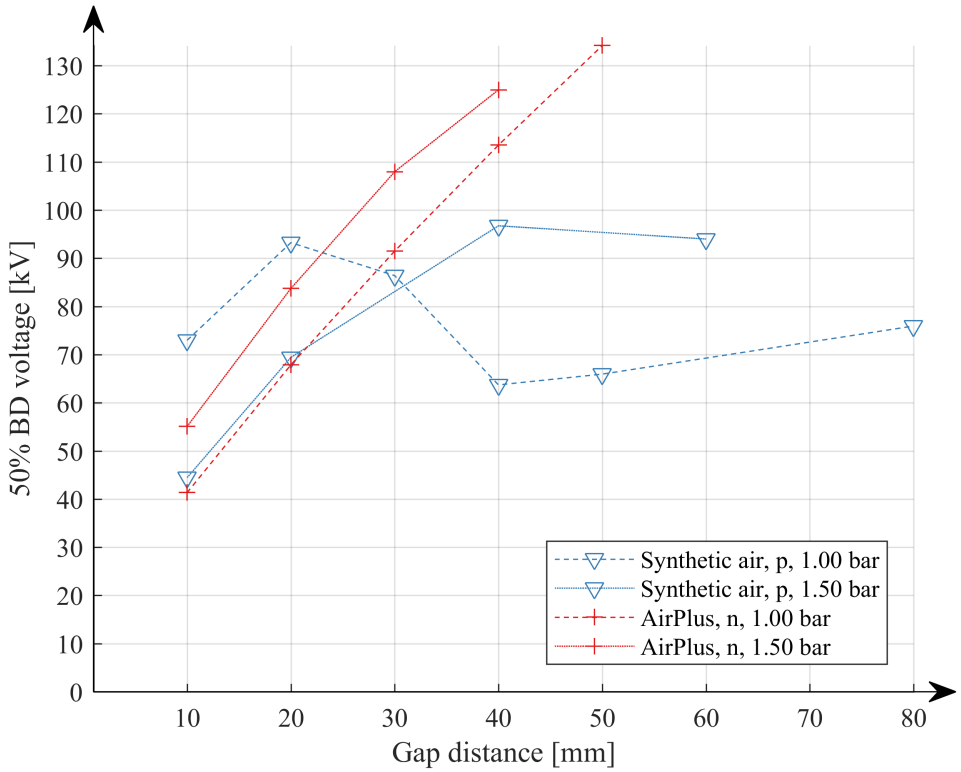

Figure 4.14: Comparison of $U_{50\%}$ as a function of gap length for rod-plane configuration with the 2.5 mm rod.

In very inhomogeneous fields and small gap lengths, synthetic air in Fig. 4.14 produces unexpected results at 1.00 bar. Here, it results in the highest $U_{50\%}$ both compared with the same results at 1.50 bar and the results for AirPlus. At these gap lengths, it is therefore difficult to compare the withstand capabilities of AirPlus and synthetic air at 1.00 bar. When the pressure is increased to 1.50 bar, the unexpected behaviour at 1.00 bar disappears for the smallest gap lengths.

4.3.5 Summary

For the results with an expected standard deviation between $0.5\Delta U$ and $2.0\Delta U$, and theoretical behaviour (increasing $U_{50\%}$ for increasing gap length and pressure), it is quite clear that AirPlus performs better than synthetic air at the investigated pressure and configurations. The measured values that contradicts this are characterised by high standard deviations and do not follow expected theoretical rules. This is especially typical for the 2.5 mm rod at 1.00 bar pressure. As the results for the homogeneous field distribution (plane-plane) is considered to be the most reliable, AirPlus is expected to have twice the withstand capability to that of synthetic air for plane-plane configurations. For rod-plane configuration, the critical flashover voltage is roughly 30% larger in AirPlus than in synthetic air.

4.4 Standard deviation

The results from $U_{50\%}$ as a function of gap distance include some large deviations from expected values, especially for the smallest rod (2.5 mm radius). The unexpectedness of the results are reflected in the standard deviations presented in Table A.4 in Appendix A. The corresponding $U_{50\%}$ values should therefore be used with this in mind.

For AirPlus, the most of the test series had a step voltage in-between the recommended interval of 0.5σ and 2.0σ. Only 7 out of 60 series (including re-tests) had a standard deviation larger than 2.0σ (most are found for the smallest rods and the smallest gaps, just as for synthetic air), providing quite reliable data for AirPlus.

In synthetic air, the rod-plane configurations yielded quite unexpected results for the smallest gap distances. The large standard deviations found indicate that something unknown is influencing the results. In general, the standard deviation is much larger for synthetic air than for AirPlus.

4.5 Numerical analysis

The numerical analysis of the streamer criterion from Eq. 2.9 provides more knowledge of the streamer processes found in the experiments. Iterating the streamer inception criterion further illustrates the assumption that the rod-plane electrodes do not have large enough gap lengths (longer than 40-50 mm) to result in streamer propagation. The gaps are homogeneous enough for the streamer criterion to indicate the steamer inception voltage, yet also inhomogeneous enough to not completely predict the streamer. For the plane-plane electrodes, only the shortest gap distances (10 mm and 20 mm) resulted in a calculated streamer long enough to traverse the gap.

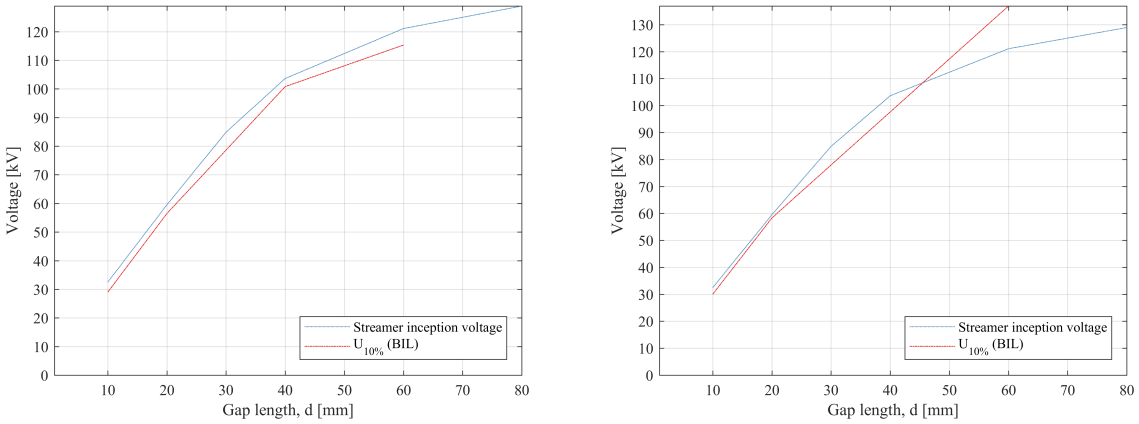

(a) Positive polarity

(b) Negative polarity

Figure 4.15: Calculated streamer inception voltage for the plane-plane configuration and the measured statistical BIL voltage.

The streamer inception calculations show that the plane-plane gap represents a homogeneous field distribution that results in $U_{50\%}$ in the streamer inception area of Fig. 2.2. The inhomogeneity factor is low enough for the field strength to be large enough to predict a streamer for 10 mm and 20 mm gap length at 1.00 bar and 10 mm, 20 mm, and 30 mm at 1.50 bar. The same calculations for the

rod-plane gaps show that the inhomogeneity is large enough to represent streamer propagation. The field strength drops below the streamer inception field, and the calculated streamer is too short for a breakdown to occur. In this area, streamer propagation is needed to explain streamer breakdown.

4.6 Sources of error

Fig. 4.14 argues for a critical look at the experimental results and procedures as the results deviate from theoretical expectations. Potential sources of error will in the following section be investigated to potentially locate the source of the deviations.

The likelihood of human sources of error has been reduced by the presence of two persons in the lab for most of the results. Such errors could be registering the wrong type of event or typing the wrong input voltage, both with likely minimal impact on the final results. Another source of human error is the adjustment of the gap distance. The adjustment was performed manually and utilised that each turn resulted in a 2 mm change of the gap. This required precise cranking as no measuring inside the tank was possible once it was sealed. To check if errors had occurred, the gap distance was measured after the tank had been evacuated to see if the final distance was indeed 10 mm for the re-test series. The error for each gap adjustment is estimated to be <0.1 mm.

4.6.1 Lightning impulse application frequency

Systematic errors can have a more severe impact on the results. One such error could be an inadequate waiting time between voltage shots. The waiting time was chosen to be 1 minute, but an extra up-and-down series was performed with 2 minute waiting time to check if this could have an impact on the measurements. This was done for the 2.5 mm rod at 1.50 bar and positive polarity. The critical flashover voltage for the re-test, performed at the end of each set-up for the 10 mm gap length, was measured to 73.6 kV with 95.4 kV standard deviation for 1 minute waiting time. Another series was therefore performed with 2 minutes of waiting time, but with no improvement on the estimation of $U_{50\%}$ and σ. $U_{50\%}$ increased to 93.3 kV, but with a reduced standard deviation of 54.2 kV. The main difference is the voltage of the first breakdown. The series otherwise inhibits the same characteristics, with no real improvement after increasing waiting time.

4.6.2 Gas quality

Another potential systematic error is the impact of breakdowns on the gas. The gas was not changed until an electrode is completely tested, so the last test series was performed in a gas that had experienced roughly 100-120 breakdowns. To investigate the potential alteration of gas composition, a re-test was performed for all series with more than one gap length investigated. The numerical values are found in Appendix B. These re-tests generally resulted in higher $U_{50\%}$ than the first test. The tests in-between could therefore be expected to perhaps be higher than if tested first. One explanation could be a change in gas mixture, resulting in gas components with higher dielectric strength than the original mixture. An analysis of the gas composition (Fig. 4.16) before and after breakdown testing was therefore performed. The results of the analysis found in Fig. 4.16 showed no indication

of gas decomposition. The amount of oxygen, nitrogen, and ozone was also measured before and after. The results found in Appendix D showed no significant change in the mole fractions for each gas. For the initial tests in synthetic air with aluminium rods (before using brass), the gas was changed to

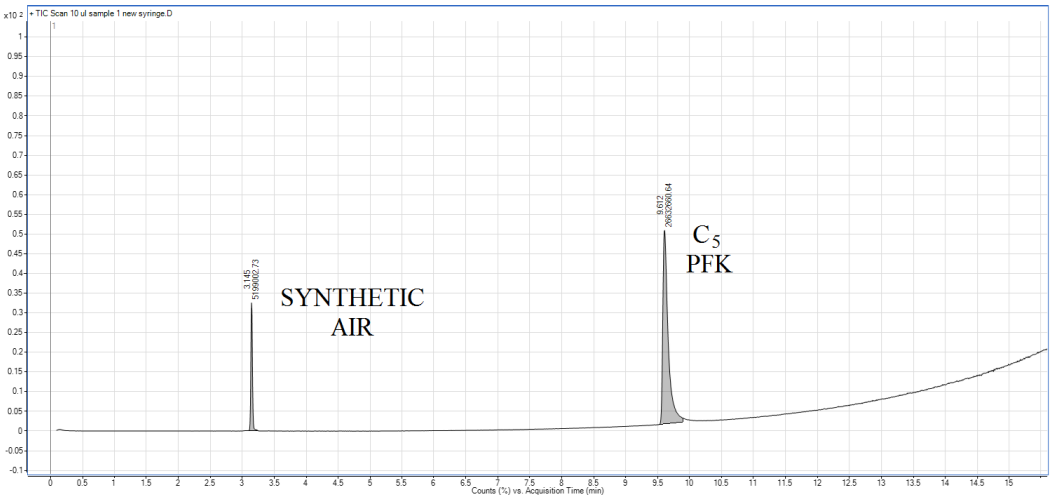

(a) AirPlus before up-and-down testing.

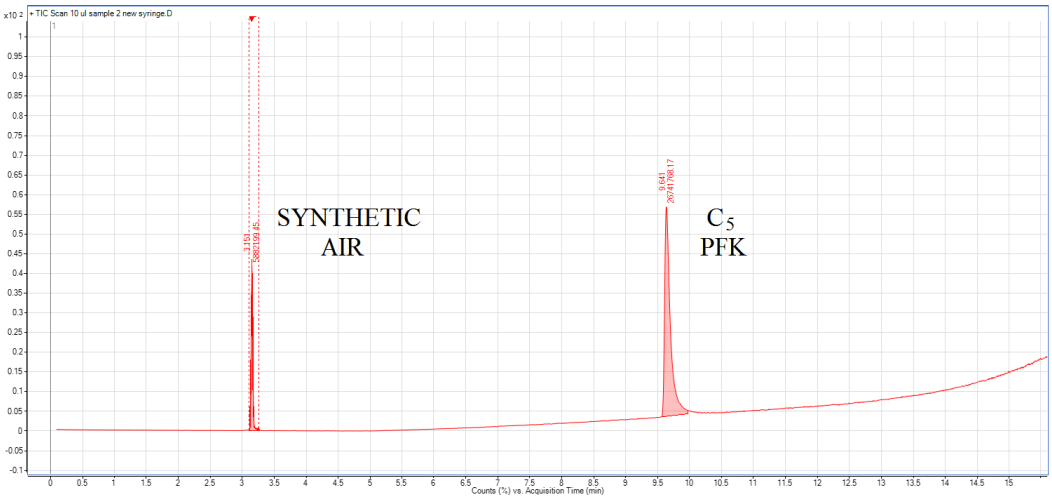

(b) AirPlus after up-and-down testing.

Figure 4.16: The change in gas composition after tests performed at 1.50 bar for the 10 mm rod.

investigate if the large values at 10 mm for the smallest rod could be explained by an alternation of the gas. The first measurements were 41.1 kV with 8.3 kV in standard deviation. The re-test jumped to 74.7 kV with a standard deviation of 86.0 kV, leading to the change of gas. After changing the gas, $U_{50\%}$ decreased to 57.0 kV with a standard deviation of 25.2 kV. This is a substantial reduction from the re-test, but the values are still quite high.

4.6.3 Electrodes

Surface decomposition was also investigated as a plausible cause for the unexpected results in Fig. 4.4 for the smallest rod in synthetic air. The surface roughness was unfortunately not possible to acquire, but visual inspection showed that it is a highly unlikely cause. The effect of a complete test for the

10 mm brass rod can be seen in Fig. 4.17. There is a clear impact on the surface, but no noticeable increase in surface roughness can be felt. Initial tests were performed using aluminium rods, but after changing to brass no noticeable impact on the estimation of $U_{50\%}$ was found.

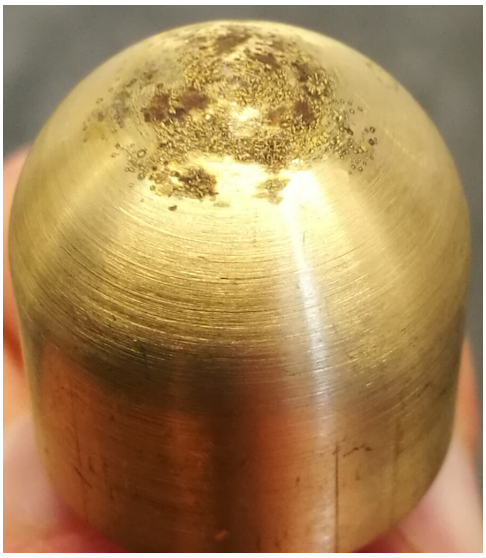

Figure 4.17: Surface decomposition after completing all up-and-down tests for the 10 mm brass rod.

4.6.4 Gas condition

In atmospheric air, it is possible to make atmospheric corrections for the impact of pressure, humidity, and temperature on $U_{50\%}$. For technical air with a humidity below 2 ppm as well as for AirPlus, no correction could be found. The pressure is kept as constant as possible, but the temperature is controlled by the room temperature. The temperature is directly proportional to the mean free path of the molecules, and will therefore impact the critical flashover voltage (E. Kuffel, Zaegel, and J. Kuffel 2000). The higher the temperature, the lower the measured critical flashover voltage. For all test series, the temperature is in the interval [19.1°C, 22.1°C] with an average value of 21.1°C.

The density of AirPlus was also recorded, but no significant deviation from 1.92 $gm^{-}3$ at 1.00 bar or 2.85 $gm^{-}3$ at 1.50 bar was measured. The same is true for the recorded pressure.

4.7 Re-testing of initial gap length

For each test set-up (polarity, pressure, electrode, gas), the first gap length, i.e. the 10 mm gap, was re-tested to investigate a systematic change in $U_{50\%}$ and s. The results showed a tendency towards an increase in the estimate for $U_{50\%}$ with an average increase of 6.2%. Separating each gas shows an interesting result. For AirPlus, only an average of 1.8% increase was measured, while for synthetic air the increase is as much as 10.6%. This could indicate that AirPlus is much less affected by the LI applications. It should however be noted that synthetic air experiences more LI applications than AirPlus due to the superior dielectric strength of AirPlus.

Breaking it further down for each electrode, the electrodes in AirPlus experiences a net increase below 1% except for the 5 mm rod. The 5 mm rod has a net increase of 5.0% across all tests caused by one particular re-test that resulted in a 31.4% increase and over seven times the standard deviation.

In synthetic air, there is a very clear correlation between field inhomogeneity and the voltage increase for the re-test. The 2.5 mm rod has a net increase of 18.6%, a value that is strictly decreasing with the inhomogeneity of the electrodes to a value of only 2% for the plane-type electrode.

5 Conclusion

The results from the up-and-down method with lightning impulse voltage stress shows that AirPlus is an improvement from synthetic air. The improvement is most prominent for homogeneous fields from the plane-plane configuration with a 50% larger measured $U_{50\%}$ in AirPlus compared with synthetic air. The experimental results also indicate that AirPlus might be sensitive to increased field inhomogeneity as the relative improvement from synthetic air to AirPlus is reduced as the rod radius was decreased for in rod-plane gaps. For the smallest rod (2.5 mm), and the configuration with the most inhomogeneous field distribution, the improvement in withstand voltage is reduced to 30%.

The same results also revealed a dependency on LI polarity for AirPlus. In synthetic air it is well established that positive LI results in lower values for $U_{50\%}$ than for negative LI. AirPlus on the other hand, looks to share the characteristics of SF_6 with lower values for $U_{50\%}$ for negative polarity compared with positive polarity. The difference were generally 7-10 kV or higher.

It was also found from re-testing of the 10 mm gap that AirPlus generates more consistent measurements compared to synthetic air. The average change from the first test at 10 mm to the re-test at 10 mm was a 10.6% increase for synthetic air, while the same average change was only an 1.8% increase for AirPlus. AirPlus also resulted in fewer series with large estimates for the standard deviations and fewer series that deviated from the expected theoretical behaviour. Synthetic air on the other hand showed a correlation between electrode shape and measurement consistency. The average re-test increase is 18.6% for the 2.5 mm rod in synthetic air.

An investigation of possible sources of error produced no clear explanation of the measurements that deviated from theoretical expectations (most notably the 2.5 mm rod in synthetic air). AirPlus was tested for gas decomposition after testing at 1.50 bar for the 10 mm rod, but no definite decomposition was found for either the C_5 PFK component or the synthetic air carrier gas. The gap length was also ruled out as an explanation as the adjustment of the gap has negligible uncertainty, and the manual adjustment was checked each time. The final important systematic error was the surface roughness of the electrodes. No surface analysis was available, but replacing electrodes showed no change in the measurement of $U_{50\%}$ or the standard deviation.

6 Further work

- The new gas will require extensive testing. The up-and-down method used in this thesis gave an indication on the performance of AirPlus compared with synthetic air for LI voltage stress. A verification of the results using the multilevel test or AC testing would be useful, especially in cases with high standard deviation. Other tests such as the constant-voltage test or the rising-voltage test, both requiring more voltage applications, could be used for more precise estimations of the mean value and standard deviation.

- Another topic of further research is the large uncertainty for many of the measurements at the lowest gap lengths. The estimated standard deviation as well as the estimated critical flashover voltage are extremely high, often surpassing the voltage at higher pressure or larger gap lengths. Numerous potential causes were discussed in Section 4.6 without a clear explanation. A high-speed camera to visualise the breakdown process could greatly help clarify the cause of the high withstand capability as physical phenomenon inside the tank, such an elongated streamer path, was not possible to detect in the current experiment.

- The field of streamer predictions in homogeneous fields could be extended to include AirPlus by performing more measurements in homogeneous field, making it possible to find the effective ionisation coefficient, $\overline{\alpha}$, for AirPlus.

References

Dixon, W. J. and A. M. Mood (1948). "A Method for Obtaining and Analyzing Sensitivity Data". In: Journal of the American Statistical Association 43.241, pp. 109–126. URL: ttp://www.jstor.org/stable/2280071.

Høidalen, H. K. (2016). *TET4130 Overspenninger og overspenningsvern*. Trondheim: NTNU.

Houghton, J. T. et al. (1995). *Climate Change 1995 - The Science of Climate Change*. Cambridge, New York: Cambridge University Press.

Hyrenbach, Maik and Sebastian Zache (2016). "Alternative Insulation Gas For Medium-Voltage Switchgear". In: 2016 Petroleum and Chemical Industry Conference Europe. DOI: 10.1109.

Ildstad, Erling (2016). *TET4160 Insulating Materials for High Voltage Applications*. NTNU, Department of Electric Power Engineering.

International Electrotechnical Commission (2010). *IEC 60060-1:2010 High-voltage test techniques - Part 1: General definitions and test requirements*. URL: http://www.standard.no/no/Nettbutikk/produktkatalogen/Produktpresentasjon/?ProductID=447403 (visited on 2018-02-01).

Kaveh Niayesh and Magne Runde (2017). *Power Switching Components*. Cham, Switzerland: Springer International Publishing.

Kuffel, E., W. S. Zaegel, and J. Kuffel (2000). *High Voltage Engineering: Fundamentals*. Newnes, Oxford: Butterworth-Heinemann.

Magne Saxegaard et al. (2018). "Dielectric Properties of Gases Suitable For Secondary Medium Voltage Switchgear". In: 23rd International Conference on Electricity Distribution. Lyon: Cired.

Pedersen, P. A., A. Blaszczyk, and H. Boehme (2009). "Streamer inception and propagation models for designing air insulated power devices". In: 2009 Annual Report Conference on Electrical Insulation and Dielectric Phenomena. Virginia Beach, Virginia, pp. 571–575.

Raether, H (1964). *Electron Avalanches and Breakdown in Gases*. London: Butterworth & Co. Ltd.

Simka, P. and N Ranjan (2015). "Dielectric Strength of C5 Perfluoroketone". In: The 19th International Symposium on High Voltage Engineering. Pilsen, Czech Republic: ABB Switzerland.

Walpole, Ronald E. et al. (2012). *Probability & Statistics for Engineers & Scientists*. 9th. Boston, MA: Pearson Education, Inc. ISBN: 978-0-321-62911-1.

White, Kenneth (2007). *IEEE Guide for Recommended Electrical Clearances and Insulation Levels in Air-Insulated Electrical Power Substations*. IEEE Std 1427™-2006. New York, NY: IEEE Power Engineering Society.

Wolfgang Hauschild and Wolfgang Mosch (1992). *Statistical Techniques for High-Voltage Engineering*. London, United Kingdom: Peter Peregrinus Ltd.

Zaengl, W. S. and K. Petcharaks (1994). *Application of Streamer Breakdown Criterion for Inhomogeneous Fields in Dry Air and SF6*. Vol. Gaseous Dielectrics. VII vols. New York: Springer Science+Business Media.

A Standard deviation

Table A.1: Numerical values from the up-and-down method for synthetic air. Plane-type

	Positive lightning impulse				Negative lightning impulse			
Pressure [bar]	Gap length [mm]	$U_{50\%}$ [kV]	s [kV]	s_m [kV]	Gap length [mm]	$U_{50\%}$ [kV]	s [kV]	s_m [kV]
1.00	10	32.8	3.0	0.7	10	33.5	2.8	0.7
	20	58.7	1.8	0.5	20	59.3	0.8	0.3
	40	103.3	2.0	0.5	40	101.9	3.3	0.8
	60	115.5	0.1	0.0	60	140.8	3.0	0.7
1.50	10	47.8	1.4	0.4	10	50.8	1.3	0.4
	20	89.4	0.9	0.3	20	89.3	1.3	0.4
	30	123.6	1.7	0.5	30	121.6	1.7	0.5

Table A.2: Numerical values from the up-and-down method for synthetic air. 10 mm

	Positive lightning impulse				Negative lightning impulse			
Pressure [bar]	Gap length [mm]	$U_{50\%}$ [kV]	s [kV]	s_m [kV]	Gap length [mm]	$U_{50\%}$ [kV]	s [kV]	s_m [kV]
1.00	10	47.5	82.2	24.9	10	75.6	10.9	2.8
	20	73.0	4.8	1.3	20	96.1	4.6	1.3
	40	94.4	11.0	2.8	40	117.1	3.9	1.1
	-	-	-	-	60	125.4	2.4	0.8
	80	127.5	0.4	0.1	-	-	-	-
1.50	10	59.3	10.3	2.5	10	92.1	13.3	33.9
	20	95.4	13.7	3.6	20	123.7	31.1	49.2
	30	113.8	6.6	1.7	-	-	-	-
	40	133.7	7.8	2.0	-	-	-	-

Table A.3: Numerical values from the up-and-down method for synthetic air. 5 mm

	Positive lightning impulse					Negative lightning impulse			
Pressure [bar]	Gap length [mm]	$U_{50\%}$ [kV]	s [kV]	s_m [kV]		Gap length [mm]	$U_{50\%}$ [kV]	s [kV]	s_m [kV]
1.00	10	48.5	168.4	8.1		10	76.7	18.9	4.6
	20	74.2	8.3	4.6		20	96.8	7.9	2.0
	30	-	-	-		-	-	-	-
	40	82.3	21.2	7.8		40	109.6	16.0	3.8
	50	-	-	-		-	-	-	-
	-	-	-	-		60	122.3	5.0	1.4
	80	121.0	17.3	0.6	-	-	-	-	
1.50	10	46.0	9.3	2.4		10	69.7	6.1	26.7
	20	65.7	3.4	0.9		20	98.6	29.2	37.6
	40	104.9	8.1	2.1		40	152.8	6.9	56.7
	60	139.4	29.0	7.1		-	-	-	-

Table A.4: Numerical values from the up-and-down method for synthetic air. 2.5 mm rod

	Positive lightning impulse				Negative lightning impulse			
Pressure [bar]	Gap length [mm]	$U_{50\%}$ [kV]	s [kV]	s_m [kV]	Gap length [mm]	$U_{50\%}$ [kV]	s [kV]	s_m [kV]
1.00	10	73	32.2	8.1	10	83.4	8.7	2.2
	20	93.3	19.5	4.6	20	98.4	4.7	1.3
	30	91.6	30.9	14.2	-	-	-	-
	40	69.1	48	7.8	40	113.7	6.2	2.8
	50	66	6.2	1.7	-	-	-	-
	80	75.9	1.9	0.6	60	129.0	6.3	1.6
1.50	10	44.5	28.6	7.2	-	-	-	-
	20	69.4	38.3	9.7	10	69.3	21.2	5.2
	40	96.8	6.5	1.7	20	101.4	57.3	14.5
	60	94.0	4.4	1.3	-	-	-	-

Table A.5: Numerical values from the up-and-down method for AirPlus. Plane-type

	Positive lightning impulse				Negative lightning impulse			
Pressure [bar]	Gap length [mm]	$U_{50\%}$ [kV]	s [kV]	s_m [kV]	Gap length [mm]	$U_{50\%}$ [kV]	s [kV]	s_m [kV]
1.00	10	63.0	1.8	0.5	10	64.8	1.7	0.5
	20	113.7	2.8	0.7	20	119.8	6.6	1.6
1.50	10	90.8	2.7	0.9	10	96.3	1.5	0.5

Table A.6: Numerical values from the up-and-down method for AirPlus. 10 mm rod

	Positive lightning impulse				Negative lightning impulse			
Pressure [bar]	Gap length [mm]	$U_{50\%}$ [kV]	s [kV]	s_m [kV]	Gap length [mm]	$U_{50\%}$ [kV]	s [kV]	s_m [kV]
1.00	10	93.4	12.8	3.1	10	74.5	9.8	2.5
	20	110.0	6.8	1.8	20	106.6	13.0	3.2
	30	116.1	4.6	1.3	30	119.5	6.3	1.7
	40	136.8	3.3	1.0	40	112.8	41.9	10.6
1.50	10	102.3	13.6	3.3	10	88.1	5.5	1.5
	20	136.1	3.3	1.0	20	127.8	5.5	1.5

Table A.7: Numerical values from the up-and-down method for AirPlus. 5 mm rod

	Positive lightning impulse				Negative lightning impulse			
Pressure [bar]	Gap length [mm]	$U_{50\%}$ [kV]	s [kV]	s_m [kV]	Gap length [mm]	$U_{50\%}$ [kV]	s [kV]	s_m [kV]
1.00	10	93.4	12.8	3.1	10	74.5	9.8	2.5
	20	110.0	6.8	1.8	20	106.6	13.0	3.2
	30	116.1	4.6	1.3	30	119.5	6.3	1.7
	40	136.8	3.3	1.0	40	112.8	41.9	10.6
1.50	10	102.3	13.6	3.3	10	88.1	5.5	1.5
	20	136.1	3.3	1.0	20	127.8	5.5	1.5

Table A.8: Numerical values from the up-and-down method for AirPlus. 10 mm rod

	Positive lightning impulse				Negative lightning impulse			
Pressure [bar]	Gap length [mm]	$U_{50\%}$ [kV]	s [kV]	s_m [kV]	Gap length [mm]	$U_{50\%}$ [kV]	s [kV]	s_m [kV]
1.00	10	73.9	21.9	5.2	10	41.4	5.7	1.5
	20	81.0	54.4	13.2	20	67.9	0.8	0.3
	30	111.6	7.5	2.0	30	91.5	3.7	1.0
	40	132.3	3.8	1.2	40	113.5	3.7	1.0
	-	-	-	-	50	134.2	6.4	1.6
1.50	10	66.1	25.0	6.2	10	55.1	2.2	0.7
	20	97.1	11.1	2.8	20	83.8	3.1	0.9
	30	125.8	7.5	2.0	30	108.0	4.1	1.1

B Re-testing of 10 mm gap

Table B.1: Re-testing of the plane-type electrode in synthetic air

	1.00 bar				1.50 bar			
	Positive polarity		Negative polarity		Positive polarity		Negative polarity	
	$U_{50\%}$ [kV]	s [kV]	$U_{50\%}$ [kV]	s [kV]	$U_{50\%}$ [kV]	s [kV]	$U_{50\%}$ [kV]	s [kV]
10 mm	33.8	2.8	34.4	2.2	47.8	1.4	50.8	1.3
Re-test	33.7	4.1	35.7	1.1	49.1	1.2	51.9	2.0
Deviation from initial test	-0.3 %	1.3 kV	3.6 %	-1.1 kV	2.6 %	-0.3 kV	2.1 %	0.7 kV

Table B.2: Re-testing of the 10 mm rod electrode in synthetic air

	1.00 bar				1.50 bar			
	Positive polarity		Negative polarity		Positive polarity		Negative polarity	
	$U_{50\%}$ [kV]	s [kV]	$U_{50\%}$ [kV]	s [kV]	$U_{50\%}$ [kV]	s [kV]	$U_{50\%}$ [kV]	s [kV]
10 mm	54.1	61.9	75.6	10.9	59.3	10.3		
Re-test	62.3	84.3	81.8	17.4	67.1	8.0		
Deviation from initial test	13.2 %	22.4 kV	7.6 %	6.5 kV	11.6 %	-2.3 kV		

Table B.3: Re-testing of the 5 mm rod electrode in synthetic air

	1.00 bar				1.50 bar			
	Positive polarity		Negative polarity		Positive polarity		Negative polarity	
	$U_{50\%}$ [kV]	s [kV]	$U_{50\%}$ [kV]	s [kV]	$U_{50\%}$ [kV]	s [kV]	$U_{50\%}$ [kV]	s [kV]
10 mm	56.3	104.0	81.0	7.7	46	9.3		
Re-test	62.5	76.7	86.1	10.3	59.2	23.8		
Deviation from initial test	9.9 %	-27.3 kV	5.9 %	2.6 kV	22.3 %	14.5 kV		

Table B.4: Re-testing of the 2.5 mm rod electrode in synthetic air

	1.00 bar				1.50 bar			
	Positive polarity		Negative polarity		Positive polarity		Negative polarity	
	$U_{50\%}$ [kV]	s [kV]	$U_{50\%}$ [kV]	s [kV]	$U_{50\%}$ [kV]	s [kV]	$U_{50\%}$ [kV]	s [kV]
10 mm	73.0	32.2	83.4	8.7	37.8	15.7	77.9	27.4
Re-test	80.2	10.3	84.6	8.7	73.6	95.4	91.9	19.8
Deviation from initial test	9.0 %	-21.9 kV	1.4 %	0.0 kV	48.6 %	79.7 kV	15.2 %	-7.6 kV

Table B.5: Re-testing of the plane-type electrode in AirPlus

	1.00 bar				1.50 bar			
	Positiv polaritet		Negativ polaritet		Positiv polaritet		Negativ polaritet	
	$U_{50\%}$ [kV]	s [kV]	$U_{50\%}$ [kV]	s [kV]	$U_{50\%}$ [kV]	s [kV]	$U_{50\%}$ [kV]	s [kV]
10 mm	63.0	1.8	64.8	1.7	90.8	2.7		
re-test	60.9	3	65.6	2	95.5	3.3		
Deviation from initial test	-3.4 %	1.2 kV	1.2 %	0.3 kV	4.9 %	0.6 kV		

Table B.6: Re-testing of the 10 mm rod electrode in AirPlus

	1.00 bar				1.50 bar			
	Positiv polaritet		Negativ polaritet		Positiv polaritet		Negativ polaritet	
	$U_{50\%}$ [kV]	s [kV]	$U_{50\%}$ [kV]	s [kV]	$U_{50\%}$ [kV]	s [kV]	$U_{50\%}$ [kV]	s [kV]
10 mm	97.7	11.9	74.53	9.8	102.3	13.6	88.1	5.5
re-test	102.5	18.5	67.6	24.9	113.4	25.4	85.4	5.7
Deviation from initial test	4.7 %	6.6 kV	-10.3 %	15.1 kV	9.8 %	11.8 kV	-3.2 %	-0.2 kV

Table B.7: Re-testing of the 5 mm rod electrode in AirPlus

	1.00 bar				1.50 bar			
	Positiv polaritet		Negativ polaritet		Positiv polaritet		Negativ polaritet	
	$U_{50\%}$ [kV]	s [kV]	$U_{50\%}$ [kV]	s [kV]	$U_{50\%}$ [kV]	s [kV]	$U_{50\%}$ [kV]	s [kV]
10 mm	102.8	14.8	67.2	12.6	71.3	6.3	66.7	5
re-test	92.1	60.6	66.2	13.7	103.9	45.9	70.6	4.8
Deviation from initial test	-11.6 %	45.8 kV	-1.5 %	1.1 kV	31.4 %	39.6 kV	5.5 %	-0.2 kV

Table B.8: Re-testing of the 2.5 mm rod electrode in AirPlus

	1.00 bar				1.50 bar			
	Positiv polaritet		Negativ polaritet		Positiv polaritet		Negativ polaritet	
	$U_{50\%}$ [kV]	s [kV]	$U_{50\%}$ [kV]	s [kV]	$U_{50\%}$ [kV]	s [kV]	$U_{50\%}$ [kV]	s [kV]
10 mm	74.8	19.7	41.4	5.7	66.1	25	55.1	2.24
re-test	81.5	19.75	40.3	5.2	63.2	11.6	55.2	2.3
Deviation from initial test	8.2 %	0.1 kV	-2.7 %	-0.5 kV	-4.6 %	-13.4 kV	0.2 %	0.1 kV

C Inhomogeneity factors the gap configurations

Table C.1: Inhomogeneity factor for each electrode ang gap length analysed

Gap length [mm]	r = 2.5 mm	r = 5 mm	r = 10 mm	Plane-type
10 mm	3.63	2.39	1.72	1.09
20 mm	5.18	3.30	2.26	1.23
30 mm	6.16	3.89	2.63	1.39
40 mm	6.83	4.33	2.88	1.58
60 mm	7.97	5.01	3.35	2.07
80 mm	9.00	5.62	3.76	2.60

D Gas analysis

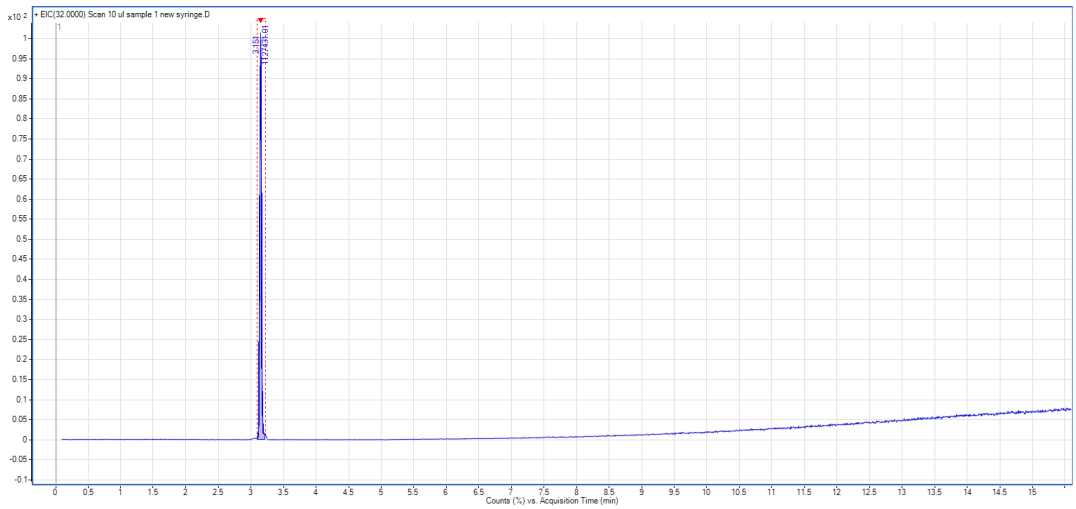

(a) Oxygen in AirPlus before up-and-down testing

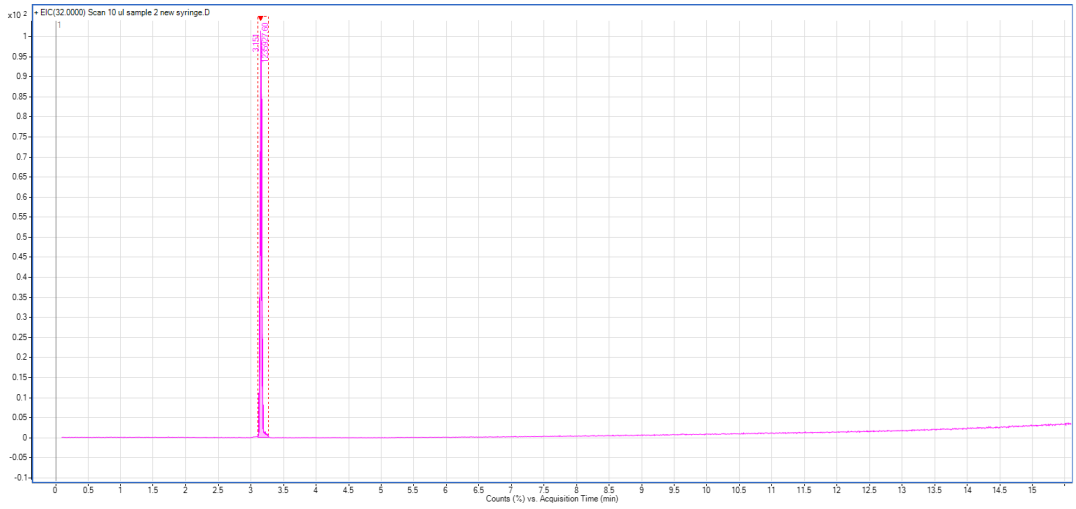

(b) Oxygen in AirPlus after up-and-down testing

Figure D.1: The change in amount of oxygen after tests performed at 1.50 bar for the 10 mm rod.

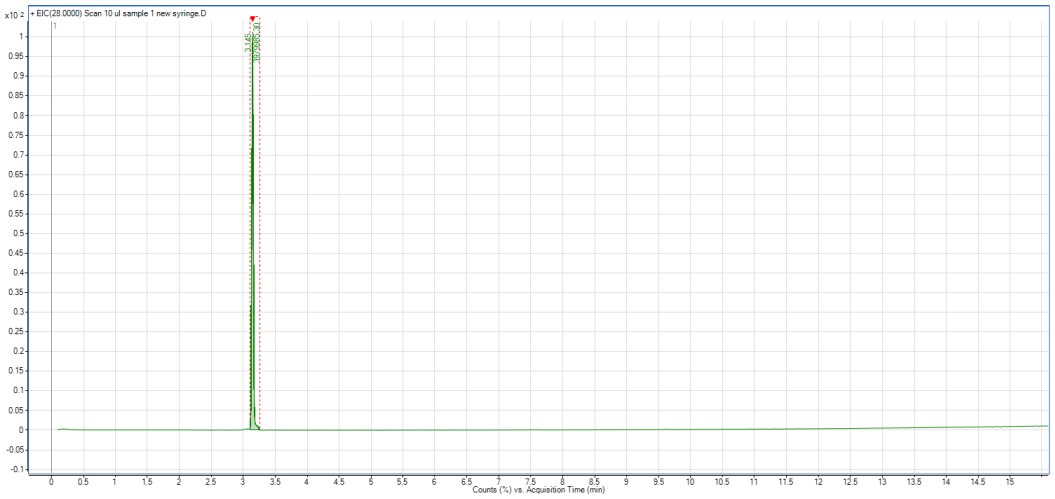

(a) Nitrogen in AirPlus before up-and-down testing

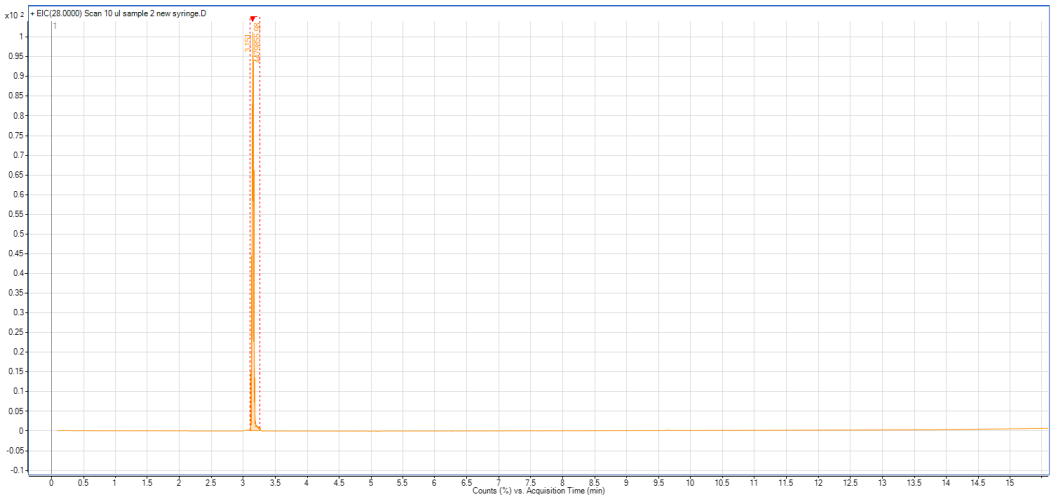

(b) Nitrogen in AirPlus after up-and-down testing

Figure D.2: The change in amount of nitrogen after tests performed at 1.50 bar for the 10 mm rod.

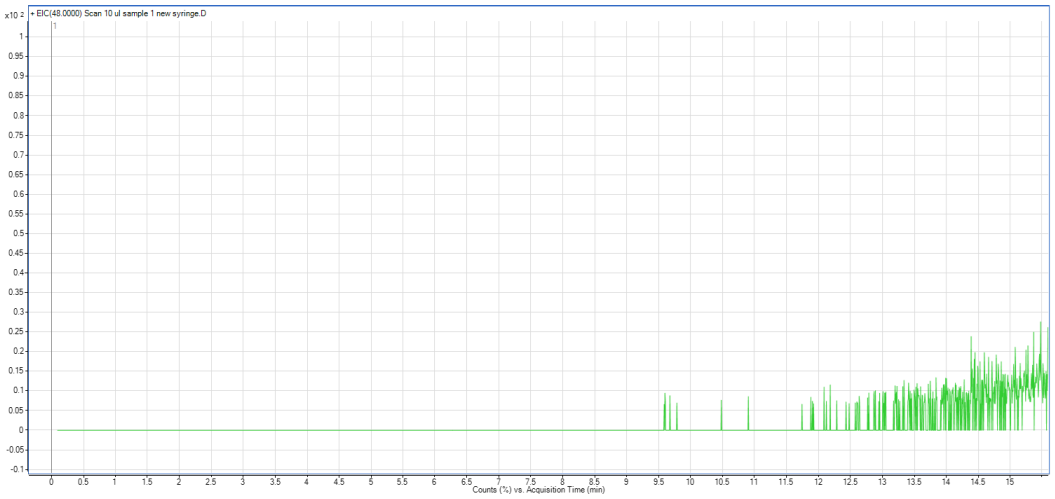

(a) Ozone before up-and-down testing

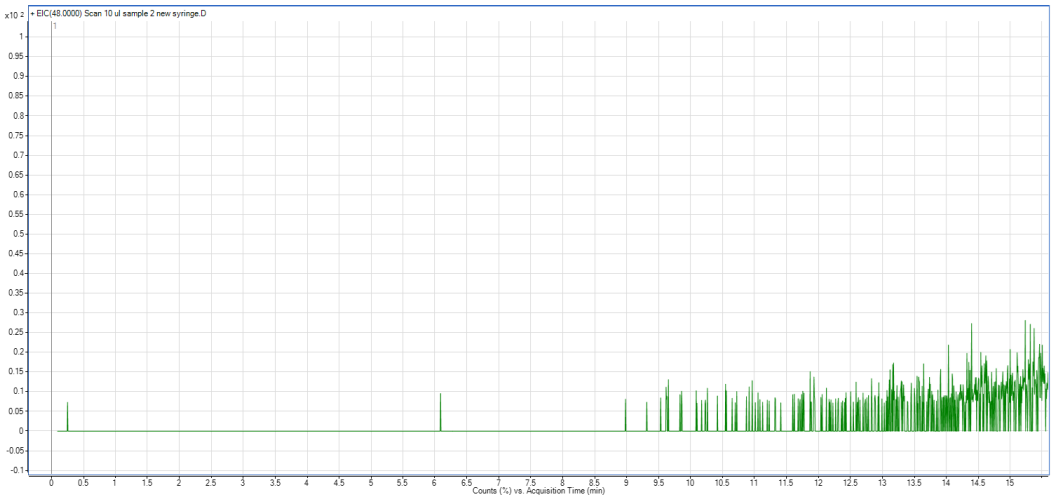

(b) Ozone after up-and-down testing

Figure D.3: The presence of ozone after tests performed at 1.50 bar for the 10 mm rod.

E MATLAB script to calculate streamer inception

The following MATLAB scripts are modifications of the scripts made by Jonathan S. Jørstad in his master's thesis "Effect of Barriers in Air Insulated Rod-Plane Gaps".

```
function [U, streamer_length, I, FieldLineNumber, E_min] = ...
    inceptionVoltageCalculate(raw_matrix, N_crit, p)
%This function calculates the streamer inception voltage from a ?x4 ...
    matrix
%on the form "r z streamline E" where r and is in mm, streamline is the
%field line number from COMSOL, and E is the electrical field in (r,z).

E_crit = raw_matrix;
U_new = 10000;      %[V]
U_prev = U_new;
U_rod = 1000;       %Electrode voltage used in COMSOL

streamer = 0; %

%Increase the voltage until a streamer is found or the limit is reached
while ¬streamer
    E_crit_scale = scaleField(E_crit, U_rod, U_new);
    [I, streamer_length, FieldLineNumber] = ...
        integrateAlpha(E_crit_scale, p);

    if I > N_crit
        streamer = 1;
    elseif U_prev > 400000
        fprintf('Error No streamer inception at 400 kV. Aborting ...
            search.')
        U = U_prev;
        return
    else
        U_prev = U_new;
        U_new = U_prev + 1000;
        streamer = 0;
    end
end

fprintf('Streamer inception found at %dkV\n',U_prev/1000)

U_upper = U_new;
U_lower = U_prev;
finished = 0;

%Calibrate U until the integral is exactly N_crit
```

```
while ¬finished
    U_test = (U_upper + U_lower)/2;
    E_crit_scale = scaleField(E_crit, U_rod, U_test);
    [I, streamer_length, FieldLineNumber] = ...
        integrateAlpha(E_crit_scale, p);

    if I > N_crit
        U_upper = U_test;
    else
        U_lower = U_test;
    end

    if floor(U_upper) == floor(U_lower)
        finished = 1;
    end

end

%Find the number of elements in one streamline
i = 1;
count = 0;
while raw_matrix(i,3) == 0
    count = count + 1;
    i = i + 1;
end
E_crit_scale(1,3)
E_streamer = zeros(length(count),1);
for i = 1:count
E_streamer(i) = E_crit_scale(i,4);
end
E_min = min(E_streamer)
U = U_test
end
```

```
function [Max_streamer, Length_max_streamer, FieldLineNumber] = ...
    integrateAlpha(raw_data, p)
%This function integrates alpha for each field line and finds the largest
%streamer with corresponding streamer length and field number.

gas = 'Air';
%Preallocating
matrix_size = size(raw_data,1);
I = zeros(101,1);
streamer_length = zeros(101,1);
j = 1;

%Iterate through field lines
for i = 0:raw_data(end,3) %Finds the last streamline

    %Preallocating
    I_matrix = zeros(matrix_size,1);
    step_matrix = zeros(matrix_size,1);

    %Integrate over a field line
    while i == raw_data(j,3)
        switch gas

            case 'Air'
                if raw_data(j,4) ≥ 2.588 && raw_data(j,4) ≤ 7.943
                   step_matrix(j) = steplength_calc(raw_data,j);
                   I_matrix(j) = ((1.6053*(raw_data(j,4)./...
                       p - 2.165)^2-0.2873)*step_matrix(j)).*p;

                elseif raw_data(j,4) > 7.943
                   step_matrix(j) = steplength_calc(raw_data,j);
                   I_matrix(j) = ((16.7766*raw_data(j,4)./...
                       p-80.006)*step_matrix(j)).*p;

                end %If

            case 'SF6'
                if raw_data(j,4) ≥ 2.588 && raw_data(j,4) ≤ 12.36
                   step_matrix(j) = steplength_calc(raw_data,j);
                   I_matrix(j) = (27.9*(raw_data(j,4)./...
                       p - 8.9246)*step_matrix(j)).*p;

                elseif raw_data(j,4) > 12.36 %
                   step_matrix(j) = steplength_calc(raw_data,j);
                   I_matrix(j) = ((22.3595*raw_data(j,4)./...
                       p-180.1709)*step_matrix(j)).*p;
```

```
                    end %If
                otherwise
                    fprintf('Error. Invalid gas.\n')
            end %Switch

            j = j+1;

            if  j == (matrix_size(1,1) + 1) %End-of-matrix.
                break
            end
        end

            %Store data from field line nr. i.
            streamer_length(i+1) = sum(step_matrix);
            I(i+1) = sum(I_matrix);

    end

    [Max_streamer,Index] = max(I(:));
    Length_max_streamer = streamer_length(Index);
    FieldLineNumber = Index-1;

    end
```

```
function E_crit_temp = scaleField(in_matrix, U_old, U_new)
%SCALEFIELD scales the electrical field strength of a streamer matrix to
%fit a new applied voltage.
matrix_size = size(in_matrix);
E_crit_temp = in_matrix;

for i = 1:matrix_size(1,1)
    E_crit_temp(i,4) = in_matrix(i,4)*U_new/U_old;
end
end
```

```
function step_length = steplength_calc(x,i)

    %Test for end-of-matrix
    if (x(i,1) == x(end,1)) && (x(i,2) == x(end,2))
        step_length = 0;
    else
        %Test for end of streamline
        if x(i,3) ≠ x(i+1,3) %End of streamline

            step_length = 0;

        else                    %Continue
            step_length = sqrt((x(i+1,1)-x(i,1))^2 + ...
                (x(i+1,2)-x(i,2))^2);
        end

     end
end
```